

Predicting the CMB power spectrum for binary polyhedral spaces

Jesper Gundemann

Danish Environmental Protection Agency, Strandgade 29, DK-1401 K

Abstract. The COBE and the first-year WMAP data both find the CMB quadrupole and octopole to be anomalously low. Here it is shown, that a finite, multi-connected universe may explain this anomaly, supporting earlier analyses [5] [18]. A novel technique, pioneered by [16] is used to compute the spectrum and its variance up to $k=102$. Based on the properties of the Lie group of rotations of S^3 it is shown that the spectrum and its variance may be computed solely from the matrix elements of the group-averaging operator, for each of the manifolds $S^3=I$, $S^3=O$ and $S^3=T$. Further, it is proved that the spectrum may be calculated solely from the radial function, due to the symmetry properties of the Lie-algebra, which is rigorously proven. It is shown, that if the topology of the universe is $S^3=I$ the uncertainty on the estimates for ℓ_{tot} may be improved by an order of magnitude. Finally, the paper highlights how the unavailability of an explicit probability function for the observations, given the model, is a challenge for Monte-Carlo simulations of the spaces $S^3=$ which has to be addressed in future work.

E-mail: jgu@mst.dk

1. Introduction

Both the COBE data and the first-year WMAP data find the CMB quadrupole and octopole to be anomalously low [1, 2]. A finite, multi-connected universe may explain this anomaly; see [4] for a review. While studies of flat spaces such as the 3-torus have not provided a good fit to the observed CMB power spectrum, a preliminary study of the so-called binary polyhedral spaces^z showed an excellent fit, particularly for the dodecahedral space [5]. Unfortunately that preliminary study suffered two major weaknesses: (1) because of computational limitations it computed only the first two terms C_2 and C_3 of the power spectrum, and (2) it neglected to compute the variances of the predicted C_ℓ , making a proper statistical analysis of the results impossible. The present article resolves both those problems. A novel approach to the computation yields reliable predictions for the power spectrum from C_2 through C_{15} , along with their respective variances.

^z See [6] for an elementary introduction to spherical spaces $S^3=$, including the binary tetrahedral, binary octahedral and binary icosahedral spaces.

For each binary polyhedral space $S^3 = \mathbb{R}^3 / \Gamma$, the computation finds the eigenmodes of the Laplacian on S^3 that are invariant under the action of the group Γ . These Γ -invariant eigenmodes define the basic modes of the primordial density fluctuations, before the decoupling of the CMB. Exploiting the symmetry properties of these eigenmodes, expressions for the CMB anisotropy and the variance of the CMB anisotropy are derived, that can be computed solely from the radial functions and the matrix elements $\langle k | G | j \rangle$ of the group-averaging operator G , which projects the space of eigenfunctions on S^3 down to the eigenspace of $S^3 = \mathbb{R}^3 / \Gamma$. For the binary polyhedral spaces $S^3 = \mathbb{R}^3 / \Gamma$, $S^3 = \mathbb{R}^3 / \Gamma$ and $S^3 = \mathbb{R}^3 / \Gamma$, the author has carried out the computations up to $k = 100$ in the space of 3-dimensional modes, yielding the estimates for the CMB anisotropy and their variances up to $l = 15$.

The ultimate goal of this work is, of course, to compare predictions to observations. Here two issues arise. The first is the question of what spectrum to use for the initial density fluctuations. The present study adopts the neutral choice of a scale-invariant initial spectrum, keeping in mind that the justification for such a choice is tenuous in a small universe and may be subject to future revision. The second issue is the reliability of the observed low- l CMB. Several authors have found unsettling alignments between the low- l modes and the ecliptic plane [7, 8], suggesting either some hitherto unknown solar system effect on the CMB or perhaps some errors in the collection and analysis of the data. In light of these uncertainties (and the significant revisions they may force onto the low- l power spectrum) it seems prudent to wait for the second-year WMAP data as well as a plausible resolution of the strange solar system alignments before drawing any conclusions about which topologies best fit observations.

2. Methods

The space-time metric for the universe in case of both the S^3 and the $S^3 = \mathbb{R}^3 / \Gamma$ models are given by the line-element

$$ds^2 = c^2 dt^2 - R(t)^2 dr^2 = a(\eta)^2 (d\eta^2 - dr^2) \quad (1)$$

where

$$dr^2 = dw^2 + dx^2 + dy^2 + dz^2 \quad (2)$$

is the spatial distance on the 3-dimensional unit sphere S^3 , $w^2 + x^2 + y^2 + z^2 = 1$, and $R(t) = a(\eta)$ is the cosmic scale factor as a function of time respectively conformal time.

The evolution of the scale factor is given by the matter dominated Friedmann-equation (see [1])

$$\frac{H}{H_0}^2 = \Omega_{\text{mass}} x^{-1} + \Omega_{\text{tot}} x^2 + 1 \quad (3)$$

where $H = \dot{a}/a$, $x = a/a_0$ is the ratio of the scale factor to the scale factor today and $H_0 = \dot{a}|_{t=t_0} / a|_{t=t_0}$. Here \dot{a} means the derivative of a with respect to the conformal time, and $\Omega_{\text{tot}} = \Omega_{\text{mass}} + \Omega_{\text{vac}}$ is the value of the total energy-density today, expressed

relative to the critical density needed to close the universe, which has contributions from both matter (baryons and cold dark matter) and from the cosmological term.

According to the current understanding, the observed variations in the CMB temperatures arises as a consequence of background fluctuations in the gravitational field, which arose during the inflationary phase, coupled to density variations in the early universe. After the universe became transparent to electromagnetic radiation, the radiation coming to the observer from the last scattering surface, will have a fingerprint from the gravitational field, as well its value at the point from where it was originally emitted, as from the value of the (changing) field, during its travel to the observer. Radiation originating at a low gravitational potential, will be more redshifted from climbing out of the lower potential, and hence be seen as cooler, than radiation originating from a local area with a high potential. And radiation experiencing a larger than average dilation effect from expansion during its travel to the observer will likewise be seen as more red-shifted than the average. The first effect is known as the "Sachs-Wolfe effect", the second as the "integrated Sachs-Wolfe effect". Following [9] we get the following temperature fluctuations:

$$T(\eta) = \frac{1}{3} [\delta_{LSS}; (\eta_{LSS})] + 2 \int_{LSS}^{\eta_0} \frac{\delta \Phi; (\eta_0, \eta)}{\eta} d\eta \quad (4)$$

This equation does not include a third effect, the Doppler-effect, which arises from the relative movement towards the observer, of the matter in the region of last scattering.

The gravitational field here, has its origin in the following ansatz for a perturbed space-time metrics:

$$ds^2 = a^2(\eta) [(1 + 2\delta\eta) d\eta^2 + (1 - 2\delta\eta) \delta_{ij} dx^i dx^j] \quad (5)$$

which is the simplest possible perturbation considering only scalar perturbations, and working in the longitudinal gauge. On large angular scales, one may ignore the effects of the anisotropic pressures generated by the metric perturbations, and find that $\delta\eta = 0$. Likewise, the influence of radiation on the metric between the last scattering surface and today may be neglected. Under these circumstances, the evolution of $\delta\eta$ is determined by

$$\ddot{\delta\eta} + 3H(1 + c_s^2) \dot{\delta\eta} - c_s^2 r^2 \delta\eta + [2H\dot{\delta\eta} + (1 + 3c_s^2)(H^2 - 1)] \delta\eta = 0 \quad (6)$$

The term with the sound velocity c_s^2 may be neglected on large angular scales, in which case we can solve the equation by the following separation ansatz:

$$\delta\eta(\eta; \mathbf{x}) = F(\eta) \sum_{j,s} X_{j,s}(\mathbf{x}) \quad (7)$$

where $X_{j,s}(\mathbf{x})$ are the eigenmodes of the Laplacian compatible with the topology S^3 of the universe, labelled with the index j , indicating the eigenvalue $-(j^2 - 1)$ of the Laplacian, and an arbitrary auxiliary numbering s of the eigenstates. The effect of the above various approximations is, that we can ignore the wavenumber dependency of

the perturbations, which reduce the dimensionality of the computational problem a lot. It is however known, that a wavenumber dependence of about 5% is found in typical models of a nearly flat space-time in the wavenumber range employed in this paper (up to $l = 101$) [10]. With the ansatz (7), we find that F satisfies [9]:

$$F'' + 3H F' + (2H' + H^2 - 1)F = 0 \tag{8}$$

where the derivatives are with respect to the conformal time η .

In the case where the primordial fluctuations are assumed to be adiabatic, as predicted from certain inflationary theories, the primordial field fluctuations are assumed to be distributed with Gaussian random complex amplitudes, on each of the eigenmodes of the Laplacian which are allowed by the topology of the universe, and with a power spectrum taken to be scale invariant (equal power per logarithmic wavenumber interval), i.e. $n_s = 1$, or almost scale invariant, $n_s \approx 1$

$$\langle X_{\mathbf{s}} \rangle = \frac{P}{n_s (2l+1)} \tag{9}$$

Here P is the overall scale of the fluctuations, whereas $X_{\mathbf{s}}$ are random complex Gaussian variables with ensemble averages

$$\langle X_{\mathbf{s}} \overline{X_{\mathbf{s}'}} \rangle = \delta_{\mathbf{s}\mathbf{s}'} \quad \langle X_{\mathbf{s}} \rangle = \langle \overline{X_{\mathbf{s}}} \rangle = \langle X_{\mathbf{s}} X_{\mathbf{s}'} \rangle = 0 \tag{10}$$

Third order moments have vanishing ensemble averages, while the only nonvanishing fourth order moment is

$$\langle X_{\mathbf{s}_1} X_{\mathbf{s}_2} \overline{X_{\mathbf{s}_3}} \overline{X_{\mathbf{s}_4}} \rangle = \delta_{\mathbf{s}_1\mathbf{s}_3} \delta_{\mathbf{s}_2\mathbf{s}_4} + \delta_{\mathbf{s}_1\mathbf{s}_4} \delta_{\mathbf{s}_2\mathbf{s}_3} \tag{11}$$

We further expand $X_{\mathbf{s}} = \int_{S^3} Y_{\mathbf{m}}(\mathbf{x})$ on the eigenfunctions to the Laplacian on S^3

$$X_{\mathbf{s}} = \int_{S^3} Y_{\mathbf{m}}(\mathbf{x}) \tag{12}$$

$$\langle X_{\mathbf{s}} \rangle = \int_{S^3} Y_{\mathbf{m}}(\mathbf{x}) \tag{13}$$

and find then from (1) the following expression for the temperature fluctuations

$$T(\eta) = \sum_{\mathbf{s}} K_{\mathbf{s}} Y_{\mathbf{m}}(\mathbf{s}; \eta) \int_{S^3} Y_{\mathbf{m}}(\mathbf{x}) \tag{14}$$

where

$$K_{\mathbf{s}} = \frac{1}{3} R_{\mathbf{s}}(LSS) + 2 \int_{LSS}^Z F^0(\eta) R_{\mathbf{s}}(\eta) d\eta \tag{15}$$

By expanding on complex basis functions and using complex random variables, we have arrived at a result which gives a complex value for the temperature fluctuations. The true fields and temperatures is of course the real part

$$2 \langle T(\eta) \rangle = \sum_{\mathbf{s}} \langle K_{\mathbf{s}} Y_{\mathbf{m}}(\mathbf{s}; \eta) \int_{S^3} Y_{\mathbf{m}}(\mathbf{x}) \rangle \tag{16}$$

The $a_{\ell m 0}$ coefficients are found from this by expanding the temperature on spherical harmonics. In the Appendix is shown that utilizing the expressions (10) for the ensemble averages of the random variables, the ensemble average of $C_{\ell m}$ may be expressed:

$$\langle C_{\ell m} \rangle = \sum_m \frac{1}{2^{\ell} + 1} \langle a_{\ell m} \bar{a}_{\ell m} \rangle = \frac{K^2 \text{trace}[G P(\ell)]}{2(2^{\ell} + 1)} \quad (17)$$

where G and $P(\ell)$ are projection operators that projects the whole eigenspace to the Laplacian belonging to the eigenvalue $\ell(\ell + 1)$ down to the eigenspace of group-symmetrical functions, and to the subspace of a particular value of the angular momentum ℓ , respectively:

$$G = \sum_s \int d\Omega \, \delta(\Omega - s) \quad P(\ell) = \sum_m \int d\Omega \, Y_{\ell m}(\Omega) Y_{\ell m}^*(\Omega) \quad (18)$$

Using that the operator G is actually a sum of right Clifford translations, and hence commutes with all left-screw transformations [12], as well as using the symmetries of the $P(\ell)$ operator it is proven in the Appendix, that the expression (17) can be simplified to

$$\langle C_{\ell m} \rangle = \sum_{\ell} \frac{K_{\ell}^2 \text{multiplicity}(\ell)}{2(2^{\ell} + 1)} \quad (19)$$

For S^3 we get just

$$\langle C_{\ell m} \rangle = \sum_{\ell} \frac{K_{\ell}^2}{2(2^{\ell} + 1)} \quad (20)$$

The significance of (19) is, that it shows that we do not have to calculate anything but the radial function, and its folding in equation (15), to calculate the spectrum, even for spaces with nontrivial topologies. The only way the topology makes the result differ from the case of S^3 is through the second factor in (19). The multiplicity (ℓ) is the dimension of the space of invariant eigenfunctions, respecting the holonomies for each eigenvalue $(\ell^2 - 1)$ of the Laplacian, and is known explicitly [11].

For the variance of the $C_{\ell m}$'s it is shown in the Appendix that it is related to the matrix elements of the group symmetrizing projection operator G as follows:

$$Q_{\ell m} = \langle C_{\ell m} \rangle \langle C_{\ell m} \rangle = \frac{1}{2(2^{\ell} + 1)} \frac{1}{2(2^{\ell} + 1)} \sum_{m m'} M_{m m'}^{\ell} \quad (21)$$

where the matrix M is derived by "symmetrizing" the sum of the matrix elements of the group averaging operator, as follows:

$$M_{m m'}^{\ell} = \sum_{\ell} K_{\ell}^2 \frac{\int d\Omega \, Y_{\ell m}(\Omega) Y_{\ell m'}^*(\Omega)}{2} \quad (22)$$

As shown in the Appendix, the matrix elements of G can be found solving a certain eigenvalue problem based on the fact that the group symmetrical functions are invariant to the holonomies of each manifold S^3/G . The matrix elements of the hermitian operator G are real, and hence symmetric. As another characteristicum, we note that all the

elements of the covariance matrix $Q_{\ell\ell}$ are non-negative. For S^3 , $G_{\ell\ell}$ is diagonal, and we recover the familiar result:

$$Q_{\ell\ell}^{S^3} = \kappa C_{\ell\ell} - \kappa C_{\ell\ell}^2 = \frac{2}{2\ell+1} C_{\ell\ell}^2 \quad (23)$$

In practical terms, we proceed as follows, which is explained further in the Appendix: For each grid point $(\ell_{\text{tot}}; m_{\text{ass}})$ in a 41 by 21 cell grid spanning the range $\ell_{\text{tot}} = 1:004$ to 1:084 and $m_{\text{ass}} = 0:2$ to 0:4, we solve the Friedmann equation (3) from $x = 1=1085$ (assuming the last scattering occurred at a redshift of $z = 1085$) and the equation (8) for F and F^0 numerically, which also supplies ℓ_{LSS} , the conformal time at the last scattering surface. Also, for each $\ell = 3:101$ and $\ell' = 2::15$ we calculate the radial wavefunction in 400 points between 0 and ℓ , using a symbolic calculator to expand the Legendre functions. Interpolating F and F^0 , we calculate the integrand in the second factor of (15) for the same 400 values of ℓ_0 . Doing then the integral by multiplication with a precalculated 400 by 400 matrix and interpolating we get both the first and the second term in (15), for each cosmic grid point. From the $K_{\ell\ell}$ values we then calculate the spectrum from (19) and the variance from (21) and (22).

From the spectrum and the variance we construct an approximate likelihood function over the $(\ell_{\text{tot}}; m_{\text{ass}})$ parameter space. The spectrum and the variance is further used to calculate the two-point angular correlation function and its variance, for each grid point.

In the Appendices, the methods and mathematical relations exploited in this work, are explained further, along with some additional results.

3. Results

The best-fit WMAP models are a natural starting point, as they incorporate a lot of constraints from the high ℓ multipoles of the spectrum. As noted in the report on the first year results from the WMAP team [3] the position of the first acoustic peak constrains the universe to be nearly flat. However, for models with a nonzero cosmological constant there is a geometric degeneracy along the lines of constant conformal distance to the last scattering surface in the $m_{\text{ass}} - \ell_{\text{tot}}$ plane, which allows models with topology S^3 or S^3/\mathbb{Z}_2 studied in this paper. Actually [3] gives as the best estimate for ℓ_{tot} the value 1.02 ± 0.02 which seems to favour a closed universe, but does not exclude either a flat universe nor an open universe. The degeneracy means, that the spectrum can be equally well fitted by assuming a flat as well as a slightly curved universe.

It is therefore assumed in this paper that the modelled spectrum of the WMAP-team coincides with the spectrum for S^3 for low ℓ 's, which is in fact verified. If the universe has a non-trivial global topology, the high ℓ behaviour is asymptotically the same if the topology is instead S^3/\mathbb{Z}_2 , provided a scaling of j_{ℓ} is applied to the spectrum of the S^3/\mathbb{Z}_2 models.

Indeed, scaling the spectrum for S^3 calculated by the methods of this paper, to the WMAP modelled spectrum (we choose to use the simple planar model here), shows a very good consistency. Applying next a relative scaling of l to the spectrum of the S^3 models studied here, we can check whether the alternative topologies can provide a better fit to the low l behaviour, while still keeping consistency with the WMAP models high l behaviour. As shown in Figure 2, the S^3 model fits equally well over the different values of l_{tot} so that the ex post likelihood distribution hardly changes the ex ante prior used (a Gaussian centred at $l_{tot} = 1.02$ with width equal to the standard deviation of l_{tot} of 0.02 reported by the WMAP team). This indicates that the procedure of scaling the overall amplitude of the modelled S^3 spectrum to the WMAP model makes sense. For $S^3=I$ and $S^3=O$, the ex post likelihood function becomes much sharper than the prior distribution, enabling us potentially to use the low multipoles to constrain the cosmological parameters more than achieved by the WMAP team, whereas the potential conclusions in the case of $S^3=T$ are more mixed. The much sharper distribution over l_{tot} especially for $S^3=I$, means that if the issue of the topology is settled, the cosmological parameters might be more strictly constrained. For $S^3=I$ the position and width of the two peaks in the likelihood occurs at $l_{tot} = 1.028 \pm 0.0023$ and for the smaller peak, at $l_{tot} = 1.017 \pm 0.0015$, almost the same value found in [10] by studying the S -statistic introduced in [3] and explained in the Appendix K of this paper. As this statistic is heavily biased to explain what we see in the observations for the lowest multipole moments, we favour instead the value 1.028 of the right peak, as the most likely estimate.

The conformal distance to the last scattering surface in the maximum likelihood peak of the map for $S^3=I$ is found to be $\chi = 0.571$ which implies that any matching circles in the sky would have a radius of

$$r = \frac{\chi}{1 - \chi^2} = 0.75 \text{ cot}(\chi) = 59.6^\circ \quad (24)$$

We could consider the topology to be a discrete cosmological parameter, and find the relative ex post probabilities for each one, by applying the Bayesian principle, as we do for the cosmological parameters. Assuming an a priori distribution of equal ex ante probability for each topology, the ex post probability, given the data, is very much in favour of the non-trivial topologies. In fact we find by such a recipe the following ex post probabilities:

$$P(S^3=I) = 0.45 \quad P(S^3=O) = 0.31 \quad P(S^3=T) = 0.13 \quad P(S^3) = 0.12 \quad (25)$$

This reasoning, however has several weaknesses. First of all, the choice of using equal a priori probabilities is a highly subjective choice. And secondly, models of inflation suggest an almost, if not completely flat Universe. Nevertheless, it is thought-provoking that the likelihood of the $S^3=I$ topology has a sharp peak very near the values of

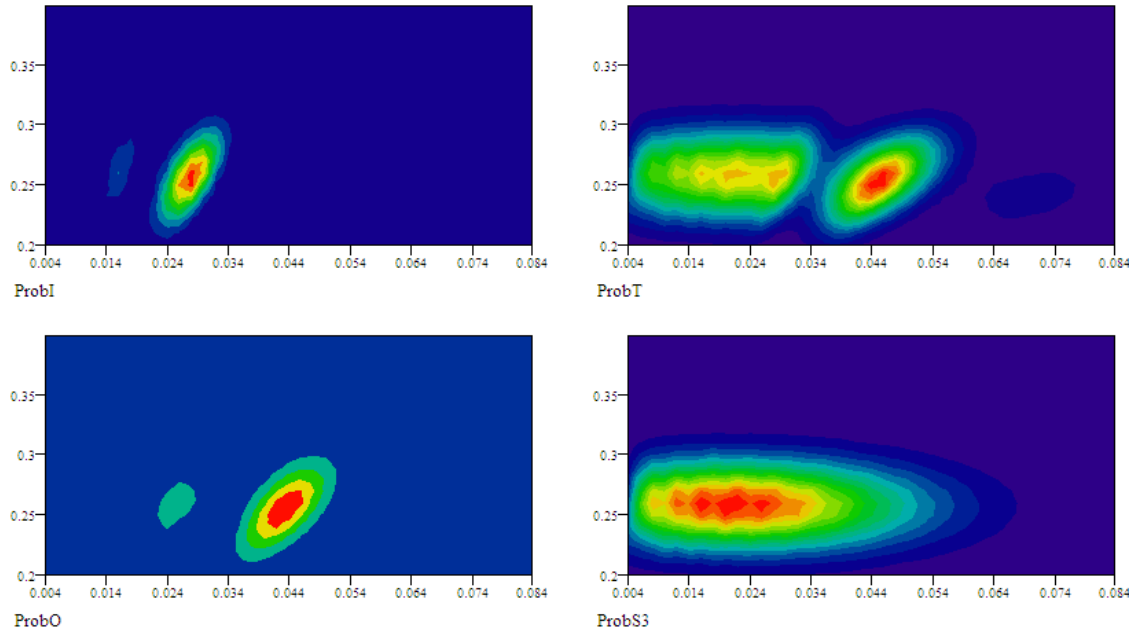


Figure 1. The ex post likelihood distribution over m_{ass} (vertical axis) and tot_1 (horizontal axis) for $S^3=I$, $S^3=T$, $S^3=O$ and S^3 , using a Gaussian prior

m_{ass} ; tot_1 found from the high l data.

In the case where we instead apply a uniform prior P^{ante} over the $(\text{tot}_1; m_{\text{ass}})$ -window, we can not assume that the modelled spectra should be scaled to the WMAP model. Instead we have to resort to scaling the spectra to the observed spectrum (which we know will produce bad results for S^3 as the low- l multipoles of the observations are systematically too low, at least if a fit to higher- l multipoles shall be realised as well). We are here bothered by the fact, that we have not in this exercise, for computational reasons, modelled the higher- l multipoles, which might more reliably make a fit between the S^3 model and data meaningful (as all topologies should approach the same curve asymptotically). Scaling nevertheless mechanically to the observed spectrum, we arrive at the results shown in Figure 3.

It is obvious, that the models $S^3=I$, $S^3=O$ and $S^3=T$ tend to have their optimum likelihood along the well-known geometrical degeneracy line of constant distance (in conformal time) to the last scattering surface. But except for $S^3=I$, the maximum likelihood regions lie at relatively improbable values of the cosmological parameters, i.e. at high m_{ass} or tot_1 , and even outside the window in parameter space studied here.

The result of this procedure is shown in Figure 4 for the case of the S^3/I topology, for the case of the so-called p_l model, which assumes a power law fit to the spectrum, using the WMAP best estimates of the m_{ass} and tot_1 for this model.

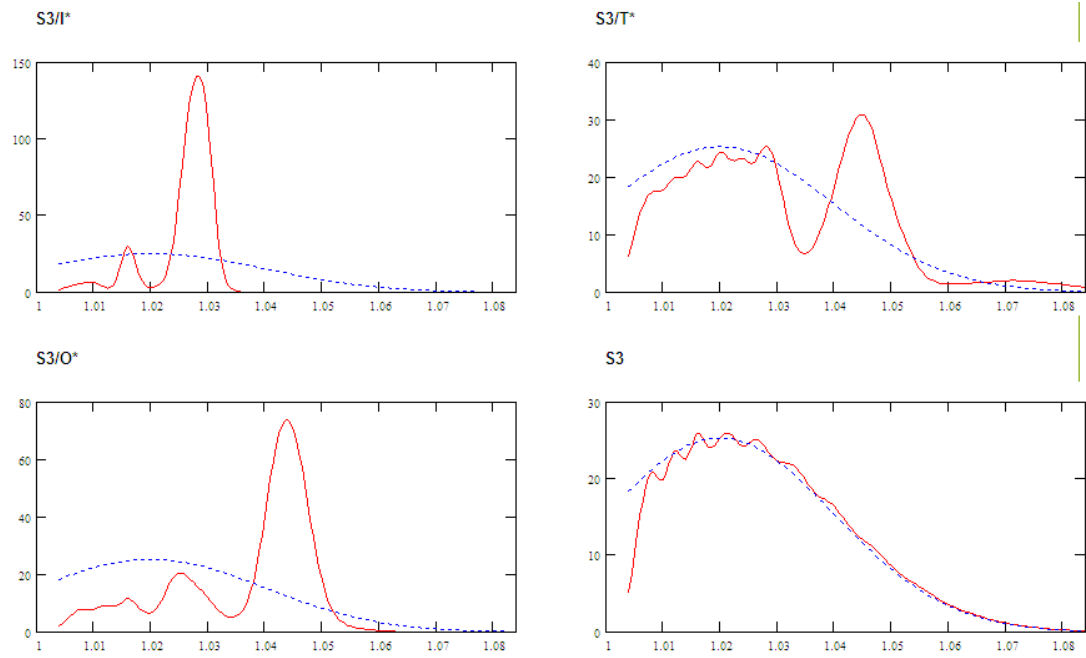


Figure 2. The likelihood distribution as a function of τ_{tot} along the most likely value of $m_{ass} = 0.26$ for $S^3=I$, $S^3=O$, S^3 and $= 0.25$ for $S^3=T$. Dotted line shows the prior distribution, for comparison. Note the different scales on the vertical axes.

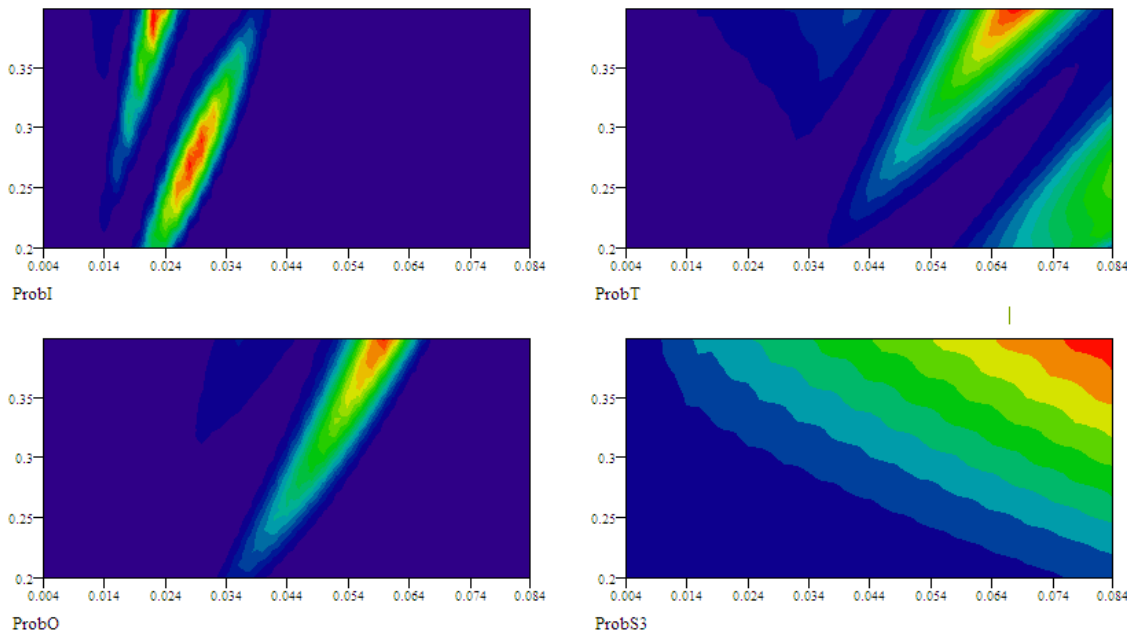


Figure 3. The ex post likelihood distribution over m_{ass} (vertical axis) and $\tau_{tot} - 1$ (horizontal axis) for $S^3=I$, $S^3=T$, $S^3=O$ and S^3 , using a uniform prior, and using best scaling to the observed multipole moments in the range of $l = 2$ to 15

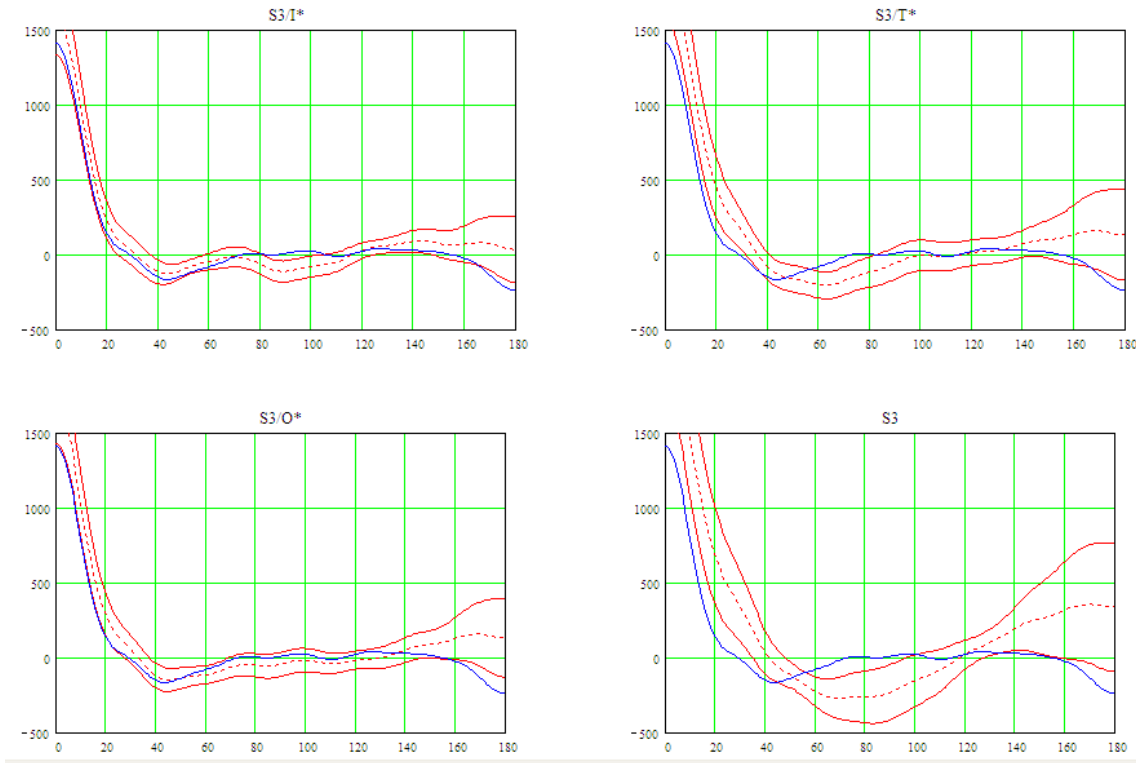


Figure 4. The temperature correlation function in the point of maximum likelihood for each of the spaces (compare Figure 1). For $S^3=I$ at $m_{ass} = 0.26$ and $tot = 1.028$, for $S^3=T$ at $m_{ass} = 0.25$ and $tot = 1.044$, for $S^3=O$ at $m_{ass} = 0.26$ and $tot = 1.044$, and for S^3 at $m_{ass} = 0.26$ and $tot = 1.016$. The graph shows the modelled ensemble average with its one standard deviation band, along with the observed correlation-function, both filtered to a maximum l of 15.

As seen, the angular correlation function is constrained almost to within one standard deviation, except around 90 degrees and near 180 degrees, which is explained solely by the very low quadrupole moment of the observations. Overall, however, the S^3/I reproduces the observed correlation function much better than the S^3 model.

This is also shown in Figure 5, showing the first 15 multipole moments, where the observed values are almost fairly well constrained to the ensemble average of the model, ± 1 times the square root of the diagonal elements of the covariance matrix, for the $S^3=I$ model, but is far outside 1 standard deviation for the S^3 model, for the $l = 2$ and $l = 11$ moments.

Acknowledgments

The author is most grateful for helpful hints from key persons in the international community working with multiconnected spaces and the CMB, inter alia Roland Lehoucq, Marc Lachieze-Rey, and Je Weeks. Especially thanks to Je Weeks, for many thoughtful comments and questions, which have helped to finalise this paper.

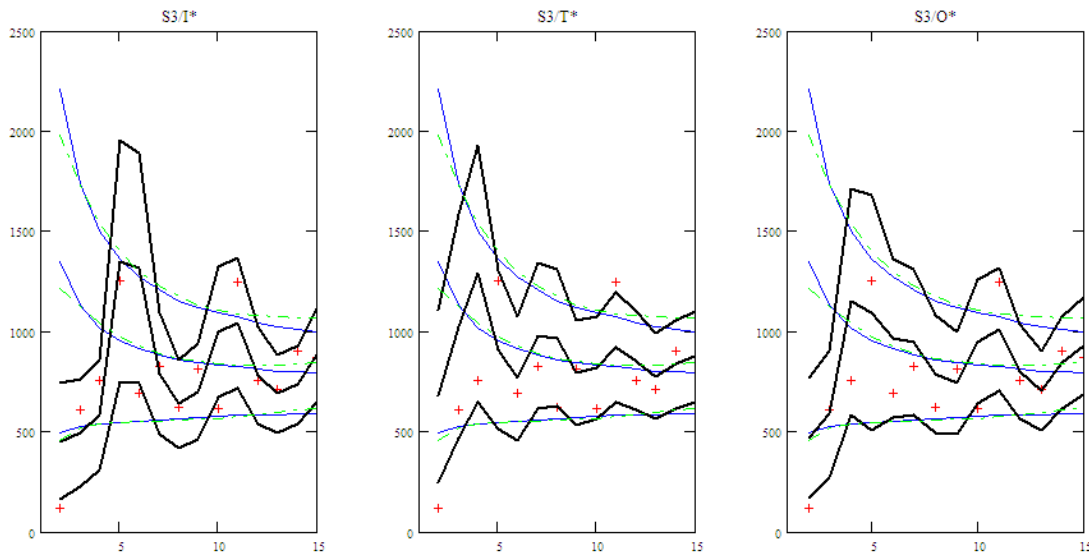


Figure 5. The spectrum for S^3/I , $S^3=T$ and $S^3=O$ for the optimum likelihood values of the cosmological parameters (as in Figure 4). Fat curves show the spectrum \pm one standard deviation (i.e. the square root of the diagonal elements of the variance-matrix). Dotted line shows the WMAP model \pm the calculated cosmological variance, and thin line shows the S^3 model \pm its standard deviation in its optimum likelihood point of parameter space. Crosses show observed multipole moments

Any errors or shortcomings remain however the sole responsibility of the author.

Appendices

Appendix A. Rotations on S^3

Rotations on S^3 can be described in complete analogy with usual rotations in E^3 , by considering the rotations to take place in the 4-dimensional Euclidian embedding space for S^3 . Working with the variables $x_n, n = 0;1;2;3$ $x = (x;y;z;w)$ a counterclockwise infinitesimal rotation of the coordinate system in the xy -plane an angle d changes the coordinates of x into x^0

$$x^0 = \begin{pmatrix} 1 & d & 0 & 0 \\ -d & 1 & 0 & 0 \\ 0 & 0 & 1 & 0 \\ 0 & 0 & 0 & 1 \end{pmatrix} x \tag{A 1}$$

A scalar function $f(x)$ transforms hereby into $f^0(x^0) = f(x)$, as follows:

$$f^0(x) = (1 + id J_{01}) f(x) \tag{A 2}$$

where J_{01} , the generator of the infinitesimal rotation, is

$$J_{01} = i \left(x \frac{d}{dy} - y \frac{d}{dx} \right) \tag{A 3}$$

Considering alternatively to be a function of the coordinates x, y, z, w ,

$$\begin{pmatrix} x \\ y \\ z \\ w \end{pmatrix} = \begin{pmatrix} \cos(\theta) \sin(\phi) \cos(\psi) \\ \cos(\theta) \sin(\phi) \sin(\psi) \\ \cos(\theta) \cos(\phi) \\ \sin(\theta) \end{pmatrix} \quad (A.4)$$

one finds that

$$J_{01} = i \frac{d}{d\theta} \quad (A.5)$$

A finite rotation of the coordinate system through the angle θ transforms as follows

$$x^0(\mathbf{x}) = e^{i J_{01} \theta} (x) \quad (A.6)$$

If instead we think of examining the value of a function at a position x^0 that arises by rotating the vector x the angle θ , i.e.

$$x^0 = R_{xy}(\theta) x \quad R_{xy}(\theta) = \begin{pmatrix} \cos(\theta) & \sin(\theta) & 0 & 0 \\ -\sin(\theta) & \cos(\theta) & 0 & 0 \\ 0 & 0 & 1 & 0 \\ 0 & 0 & 0 & 1 \end{pmatrix} \quad (A.7)$$

we can do it by rotating the coordinate system the same amount, finding the transformed function, and checking its value at the new coordinate equal to the old, i.e.

$$(R_{xy}(\theta) x) = e^{i J_{01} \theta} (x) \quad (A.8)$$

If we do two consecutive rotations we have to undo them in reverse order:

$$(R_{zx}(\theta) R_{xy}(\theta) x) = e^{i J_{21} \theta} (R_{xy}(\theta) x) = e^{i J_{01} \theta} e^{i J_{21} \theta} (x) \quad (A.9)$$

Appendix B. The Lie algebra of rotations on S^3

In the following we state some useful properties of the Lie algebra of rotations on S^3 . The generators $J_k, k = 0, 1, 2, 3$ of the rotations are hermitian and satisfy the following commutation relations:

$$[J_k, J_m] = i J_{m k} \quad (B.1)$$

for any three different indices k, m as well as

$$[J_k, J_{m n}] = 0 \quad (B.2)$$

when k, m and n are all different.

For an observer sitting in $(x; y; z; w) = (0; 0; 0; 1)$ the three generators J_{01}, J_{20} and J_{12} will be the analogue on S^3 for usual rotations around the z -, y and x -axis respectively, and the sum of their squares will be the analogue of the familiar total angular momentum L^2 .

$$L^2 = J_{01}^2 + J_{20}^2 + J_{12}^2 \quad (B.3)$$

It is useful to introduce also the right and left screw generators:

$$SR_0 = J_{12} + J_{30} \quad SR_1 = J_{20} + J_{31} \quad SR_2 = J_{01} + J_{32} \quad (B.4)$$

$$SL_0 = J_{12} - J_{30} \quad SL_1 = J_{20} - J_{31} \quad SL_2 = J_{01} - J_{32} \quad (B.5)$$

We note, that the left screw generators here are chosen with the opposite sign than if thought of as moving from $(x; y; z; w) = (0; 0; 0; 1)$ in the direction of the z-axis and simultaneously making a left-hand rotation of y towards x. This makes the following formulas more symmetric between the SR and SL set.

The screw generators satisfy the following commutation relations:

$$[SR_0; SR_1] = 2iSR_2 \quad [SL_0; SL_1] = 2iSL_2 \quad (B.6)$$

and analogous, by cyclic permutation.

Further, any pair of left and right screw generators commute:

$$[SL_k; SR_l] = 0 \quad (B.7)$$

The following operators commute with all the generators, and are thus Casimir-operators of the Lie group:

$$J^2 = J_{01}^2 + J_{02}^2 + J_{03}^2 + J_{12}^2 + J_{13}^2 + J_{23}^2 = \frac{1}{2}(SL^2 + SR^2) \quad (B.8)$$

$$SR^2 = SR_0^2 + SR_1^2 + SR_2^2 \quad (B.9)$$

$$SL^2 = SL_0^2 + SL_1^2 + SL_2^2 \quad (B.10)$$

Further, we can construct lifting operators

$$AR_2 = SR_0 + iSR_1 \quad AR_2 - AR_2 = AR_2 - SR_2 + 2 - AR_2 \quad (B.11)$$

$$AL_2 = SL_0 + iSL_1 \quad AL_2 - AL_2 = AL_2 - SL_2 + 2 - AL_2 \quad (B.12)$$

These relations (that holds also by cyclic permutation) show that AR_2 acting on an eigenstate to SR_2 with eigenvalue sr is also an eigenstate to SR_2 with eigenvalue $sr + 2$, i.e. AR_2 "lifts" the eigenvalue of SR_2 2 units, and analogously for AL_2 acting on an eigenstate to SL_2 . In a similar way, the adjoint operators are seen to lower the eigenvalue 2 units:

$$AR_2^\dagger = SR_0 - iSR_1 \quad AR_2^\dagger - AR_2^\dagger = AR_2^\dagger - SR_2 - 2 - AR_2^\dagger \quad (B.13)$$

and analogously for AL_2^\dagger .

The left screw lifting and lowering operator does not change the eigenvalue of the right screw operator and vice versa:

$$[AL_2; SR_2] = [AL_2^\dagger; SR_2] = [AR_2; SL_2] = [AR_2^\dagger; SL_2] = 0 \quad (B.14)$$

We can thus have states that are simultaneously eigenvectors to SL_2 and SR_2 , with eigenvalues in a range $s_{l_{min}}; s_{l_{min}} + 2 :::: s_{l_{max}}$ determined by the nonvanishing of the result of the lifting and lowering operations. The squared norm of a state resulting from application of the lifting operator is (we here use the Dirac-notation explained in Appendix C):

$$\langle s | sr \mathcal{A} L_2^\dagger \mathcal{A} L_2 | s \rangle = \langle s | sr \mathcal{J} L_0^2 + S L_1^2 + i[S L_0; S L_1] | s \rangle = \quad (B.15)$$

$$\langle s | sr \mathcal{J} L^2 - S L_2^2 - 2 S L_2 | s \rangle = S L^2 - s l^2 - 2 s l \quad (B.16)$$

where we have used that $S L^2$ commutes with all the generators and thus is a common eigenvalue for all the states.

Similarly, we find that the squared norm after lowering is

$$\langle s | sr \mathcal{A} L_2 \mathcal{A} L_2^\dagger | s \rangle = S L^2 - s l^2 + 2 s l \quad (B.17)$$

We thus see that the number ν_l of different eigenvalues $s l = (\nu_l - 1); (\nu_l - 1) + 2; ::::; \nu_l - 1$ is related to $S L^2$ as follows $S L^2 = \nu_l^2 - 1$. We would get the same result by examining the possible range of eigenvalues for any of the left screw operators, so the multiplet of states should also be spanned by a basis of eigenstates of the other two left screw generators as well, with ν_l different eigenvalues. A similar reasoning shows that the range of possible eigenvalues for SR_2 is $s r = (\nu_r - 1); (\nu_r - 1) + 2; ::::; \nu_r - 1$ where ν_r is the number of different eigenvalues, related to $SR^2 = \nu_r^2 - 1$.

The 2 numbers ν_l and ν_r completely characterise the multiplet, and we can easily construct a matrix representation of the operators, by choosing a basis where SL_2 and SR_2 are diagonal. The dimension of the representation is equal to $\nu_l \nu_r$. In such a representation the nonvanishing matrix elements can be chosen as

$$\langle s | sr \mathcal{J} L_2 | s \rangle = s l \quad \langle s | sr \mathcal{J} R_2 | s \rangle = s r \quad (B.18)$$

$$\langle s | sr + 2 | s \rangle \mathcal{A} L_2 | s \rangle = i \frac{q}{\nu_l^2 - s l^2 - 2 s l} = a l(s l) \quad (B.19)$$

$$\langle s | sr + 2 | s \rangle \mathcal{A} R_2 | s \rangle = i \frac{q}{\nu_r^2 - s r^2 - 2 s r} = a r(s r) \quad (B.20)$$

The above analysis illustrates that any irreducible representation of the commutator-algebra of the generators J_k , of rotations of E^4 is in fact the direct product of representations of the algebras of generators for rotating E^3 : $SO(4) = SO(3) \times SO(3)$, which is further exploited in Appendix E (see also [19] which uses this fact to derive explicit analytical solutions for the lowest eigenfunctions of the Poincare dodecahedral space). Although we can have abstract multiplets for any $\nu_r; \nu_l$, the multiplets corresponding to single component wave functions have $\nu_r = \nu_l = \nu$. One may in fact show, that the Laplacian for such wave functions is simply J^2 . There are thus ν^2 states in the multiplet, corresponding to the multiplicity ν^2 for eigenstates to the Laplacian on S^3 , with eigenvalue $(\nu^2 - 1)$. The usefulness of studying the possible choices of commuting operators is that we can use the eigenvalues of the operators to label the degenerate

eigenstates of the Laplacian on S^3 . Where the conventional choice is to use the set of operators J^2, L^2, J_{01} , we have found it useful to employ instead the set J^2, SR_2 and SL_2 .

The above explicit expressions (B.18) to (B.20) determine all the generators J_k . There is a choice of relative phases between states involved, in the choice of the lifting operators. This is purely conventional, and the expressions may be multiplied by any complex number with modulus 1. Our use of the factors of i are convenient, however, as then the operators J_{01} and J_{20} which are generators of rotations around the z -axis and y -axis respectively are both real matrices:

$$SR_0 = \frac{1}{2} (AR_2 + AR_2^y) \quad SL_0 = \frac{1}{2} (AL_2 + AL_2^y) \quad (B.21)$$

$$SR_1 = \frac{1}{2i} (AR_2 - AR_2^y) \quad SL_1 = \frac{1}{2i} (AL_2 - AL_2^y) \quad (B.22)$$

$$J_{12} = \frac{1}{2} (SR_0 + SL_0) \quad J_{20} = \frac{1}{2} (SR_1 + SL_1) \quad J_{01} = \frac{1}{2} (SR_2 + SL_2) \quad (B.23)$$

$$J_{30} = \frac{1}{2} (SR_0 - SL_0) \quad J_{31} = \frac{1}{2} (SR_1 - SL_1) \quad J_{32} = \frac{1}{2} (SR_2 - SL_2) \quad (B.24)$$

Appendix C. The eigenstates of the Laplacian on S^3

We can in fact use the rotation operators to calculate the eigenfunctions. We use the Dirac notation [13], well known from its use in quantum mechanics:

$$\langle f | j, g \rangle = \int \overline{f(\theta, \phi)} g(\theta, \phi) d\Omega \quad (C.1)$$

where $d\Omega = \sin^2(\theta) \sin(\theta) d\theta d\phi$. This expression is what physicists would call the expression for $\langle f | j, g \rangle$ in the coordinate representation. If however we have an expansion of f and g on a complete set of basis functions, call them $|j, m\rangle$, we can also calculate $\langle f | j, g \rangle$ in the following matrix representation:

$$F(j, m) = \langle f | j, m \rangle \quad G(j, m) = \langle g | j, m \rangle \quad (C.2)$$

as

$$\langle f | j, g \rangle = \sum_m \overline{F(j, m)} G(j, m) \quad (C.3)$$

or for short

$$\langle f | j, g \rangle = F^y G \quad (C.4)$$

Considering $|j, m\rangle$ to be the name of the delta-function on S^3 , we can write a scalar function as

$$f(\theta, \phi) = \sum_m |j, m\rangle \quad (C.5)$$

An eigenfunction to the Laplacian, say the $|j, m\rangle$ state, may then be calculated using the rotation operators, as follows

$$|j, m\rangle(\theta, \phi) = \langle j, 0 | j, m \rangle = \langle 0 | j, m \rangle e^{i J_{32}} e^{i J_{20}} e^{i J_{01}} |j, m\rangle \quad (C.6)$$

This expression may most easily be understood, by noting that we simply make rotations of the coordinate system in the order $j; i; j$ that has the effect that the point $(j; i; j)$ gets new coordinates $(0;0;0)$

$$j^0 = e^{i J_{32}} e^{i J_{20}} e^{i J_{01}} \quad j^0(0;0;0) = (j; i; j) \tag{C.7}$$

which is maybe easier to grasp than the alternative

$$h000j e^{i J_{32}} e^{i J_{20}} e^{i J_{01}} = h \quad j \tag{C.8}$$

which in conjugated form is

$$j \quad i = e^{i J_{01}} e^{i J_{20}} e^{i J_{32}} j000i \tag{C.9}$$

and which can be seen as the $j \quad i$ state arising from a rotation of the state $j000i$ in the sequence $j; i; j$, where there is a minus as we rotate the state, rather than the coordinate system.

How do we calculate the expression (C.6)? Well, the rule, which is so familiar in quantum mechanics, is that the only way to calculate the result of a linear operator, defined as a function of another linear operator, is to do it in a basis of eigenfunctions. So each of the above rotations must be calculated in a basis of eigenstates for the $J_{32}; J_{20}$ and J_{01} operators, respectively, making it necessary to transform between these bases.

These rotations mix the various eigenstates belonging to a beta-subspace, but do not mix states with different betas. In the calculation of the eigenfunctions we can therefore freely insert projection operators such as $\sum_{s_l s_r} \delta_{s_l s_r} j^m i^m j$ for that subspace. In that way we get from equation (C.6) (and now suppressing the $-$ index everywhere)

$$j^m(j; i; j) = \sum_{s_l s_r} h000j \sum_{s_l s_r} \delta_{s_l s_r} j^m i^m j \quad e^{i J_{32}} e^{i J_{20}} e^{i J_{01}} j^m i^m j \tag{C.10}$$

Simplifying, we get

$$j^m(j; i; j) = \sum_{s_l s_r} h000j \sum_{s_l s_r} \delta_{s_l s_r} j^m i^m j \quad e^{i J_{32}} e^{i J_{20}} e^{i J_{01}} j^m i^m j \tag{C.11}$$

We have used the diagonal character of the rotation operators, acting in their respective bases, to set indices equal, where appropriate. We have also used, that the only $j^m i^m j$ combination that gives a $j^m(0;0;0) \neq 0$ is $j^m i^m j = j^m i^m j$. Further, the value is

$$j^m(0;0;0) = h000j \sum_{s_l s_r} \delta_{s_l s_r} j^m i^m j = i \frac{s^2}{2} \tag{C.12}$$

We do not calculate (C.6) in the coordinate representation, but instead set up a matrix representation, where each state is a vector, and the operators are matrices.

As a natural twist, we can write (C.11) as

$$\begin{aligned}
 & Y_m(\theta; \phi) \\
 &= \sum_{sr} N_{sr} h_{sr} = \sum_{sr} \int_{-1}^1 \int_0^{2\pi} e^{i sr} h_{sr} = \sum_{sr} \int_{-1}^1 \int_0^{2\pi} e^{i sr} Y_m(\theta; \phi) \\
 &= R_{sr}(\theta) Y_m(\theta; \phi)
 \end{aligned} \tag{C.13}$$

where

$$N_{sr} = i^{l-s} \frac{\sqrt{2s+1}}{(2s+1)} \tag{C.14}$$

It is seen, that we have derived a Fourier expansion of the radial function $R_{sr}(\theta)$. We here used the result for S^2 , analogous to (C.6), that

$$Y_m(\theta; \phi) = \int_{-1}^1 \int_0^{2\pi} e^{i J_{20}} e^{i J_{01}} Y_m(\theta; \phi) = \int_{-1}^1 \int_0^{2\pi} e^{i J_{20}} e^{i J_{01}} Y_m(\theta; \phi) \tag{C.15}$$

where

$$h_{00} = \frac{\sqrt{2s+1}}{4} \tag{C.16}$$

Appendix D. The group symmetrical states

For the manifolds S^3 we are studying, there exist a set of Clifford translations, that connects any point to each of its ghost-images. These Clifford translations are defined as the screw-transformations that bring the origin to the images of the origin. The Universe may employ either left or right screw translations, which however is immaterial for the analysis of this paper. Here and in the following, we settle for right-screw transformations. It is convenient to imagine the observer to be situated in the "origin" $(x;y;z;w) = (0;0;0;1)$, which has angular coordinates $(\theta; \phi) = (0;0;0)$.

The coordinate transformation involved for the $x_k, k = 0;1;2;3$ is thus, for a screw-translation g which brings the origin to a point with angular coordinates $(\theta; \phi)$

$$x^0 = g(x) = R_{xy}(\theta) R_{zx}(\phi) R_{screw}(\theta, \phi) R_{zx}(\phi) R_{xy}(\theta) x \tag{D.1}$$

Here, the rotation matrices R_{xy} and R_{zx} are the usual 4x4 matrices for rotating a vector an angle θ and ϕ in the xy plane and the zx plane respectively, leaving the other two coordinates unchanged, while R_{screw} performs a right-screw transformation along the z -axis:

$$R_{screw}(\theta, \phi) = \begin{pmatrix} 0 & \cos(\theta) & \sin(\theta) & 0 & 0 & 1 \\ \cos(\phi) & \sin(\phi) & 0 & 0 & 0 & 0 \\ \sin(\phi) & -\cos(\phi) & 0 & 0 & 0 & 0 \\ 0 & 0 & \cos(\theta) & \sin(\theta) & 0 & 0 \\ 0 & 0 & \sin(\theta) & -\cos(\theta) & 0 & 0 \end{pmatrix} \tag{D.2}$$

The logic is, that first we apply a rotation of the coordinate system (first θ , then ϕ) that brings our target point to lie on the z -axis, then we do the screw, and transform back to the proper $\theta; \phi$ direction.

Instead of transforming the coordinates, we use our insights from Appendix A, equations (A.8) and (A.9), that we can alternatively find the transform of the function

$$(x^0) = \langle x^0 | j \rangle = \langle x | \mathcal{J} | j \rangle = \langle x | \mathcal{J} e^{i J_{01}} e^{i J_{20}} e^{i S R_2} e^{i J_{20}} e^{i J_{01}} | j \rangle \quad (D.3)$$

We can make the average over all the j ghost images of x , and find that it is

$$\frac{1}{j} \langle x | \mathcal{J} | j \rangle = \langle x | \mathcal{J} | j \rangle \frac{1}{j} \sum_n e^{i n J_{01}} e^{i n J_{20}} e^{i n S R_2} e^{i n J_{20}} e^{i n J_{01}} | j \rangle \quad (D.4)$$

where the sum is over all the coordinates j ; j of the ghost images of the origin. We see from this, that any group-symmetrical function ψ , for which $\langle g(x) | \psi \rangle = \langle x | \psi \rangle$ for all g , evidently is an eigenfunction to the group-averaging operator, with eigenvalue 1:

$$\langle x | \mathcal{J} | j \rangle = \langle x | \mathcal{G} | j \rangle \quad (D.5)$$

where

$$\mathcal{G} = \frac{1}{j} \sum_n e^{i n J_{01}} e^{i n J_{20}} e^{i n S R_2} e^{i n J_{20}} e^{i n J_{01}} \quad (D.6)$$

It may be shown, that the group averaging operator is in fact a projection operator, i.e. an operator with eigenvalues either 0 or 1 [11]. Finding the group symmetrical functions thus boils down to finding the eigenvectors to the matrix \mathcal{G} , that have eigenvalue 1. Denoting these j s_i where $s = 1; \dots; m$ multiplicity (m), the permissible eigenfunctions for the Laplacian on S^3 are

$$\psi_s(x) = \langle x | j \rangle s_i \quad (D.7)$$

The fact that \mathcal{G} is a projection operator means that we can write

$$\mathcal{G} = \sum_s \langle j | s \rangle s_i \langle s | j \rangle \quad (D.8)$$

The operator \mathcal{G} has many symmetries. First of all, it is evident from equation (D.6), that \mathcal{G} is a sum of right-screw Clifford-translations. As any right-screw Clifford translation commutes with any left-screw Clifford translation [12] this has the consequence, that \mathcal{G} commutes with $S L_2$ as well as the lifting-operator $A L_2$. This implies that eigenstates to \mathcal{G} may be chosen as simultaneous eigenstates to $S L_2$. Each such eigenstate will then be a superposition of states with identical left-screw eigenvalue but different right-screw eigenvalues:

$$| j \rangle s_i = \sum_{sr} \langle j | s \rangle s_i^0 = \sum_{sr} a_{s^0}^{sr} | j \rangle s_r s_l i \quad (D.9)$$

Here we can choose $a_{s^0}^{sr}$ to be independent of s_l as is easily seen by acting with the lifting operator $A L_2$ on the sum. This is seen to be consistent with the known fact that the multiplicity, i.e. the number of eigenstates for each s , is a multiple of s . Now the group-symmetrical functions must be eigenstates with eigenvalue 1 to each of the Clifford-translations in the group defining the space S^3 . Specially, if we choose our coordinate system to have its z-axis aligned along one of the basic Clifford-translations, they must be eigenfunctions with eigenvalue 1 to the screw-translations along the z-axis

over an angle $\theta = \frac{2}{N} = \frac{2}{10}; \frac{2}{8}; \frac{2}{6}$ for the case of $N = I; O; T$ respectively.

As each of the sr eigenstates is an eigenstate to such translations with eigenvalue $e^{i sr}$ we realise that the only admissible sr values in the expansion (D.9) are $sr = 0 \pmod N$.

Appendix E. The ℓ m states

We can find the simultaneous eigenvectors $|j \ell m\rangle$ of the operators L^2 and J_{01} (the conventional ℓ m set) by simply calculating the eigenvectors of the matrix $L^2 + J_{01}$ the eigenvalues of which are all different. Our software (Mathcad) then automatically supplies real eigenvectors, as the matrix is real, meaning that the transformation matrix from the jr basis to the $j \ell m$ basis becomes real. We can fix the sign of each ℓ m eigenvector, by calculating the wave function (C.6) in a single point, and comparing with the following analytical expression:

$$\langle j \ell m | i \rangle = \sqrt{\frac{2\ell+1}{4\pi}} R_{\ell}(\rho) Y_{\ell}(\theta; \phi) \tag{E.1}$$

The factor of i^m will disappear if we choose to omit the i in (27) and (28), which is the convention used in the following.

Here $Y_{\ell m}$ are the usual spherical harmonic functions, with the symmetry

$$\overline{Y_{\ell m}} = (-1)^m Y_{\ell, -m} \tag{E.2}$$

whereas the radial function R_{ℓ} has the explicit analytical expression [9]:

$$R_{\ell}(\rho) = M_{\ell} \frac{P_{\ell}(\frac{1}{2}; (\ell + \frac{1}{2}); \cos(\theta))}{(1 - \cos(\theta)^2)^{\frac{1}{4}}} \tag{E.3}$$

where the normalisation factor is

$$M_{\ell} = i^{\ell} \sqrt{\frac{2\ell+1}{4\pi} \frac{1}{\int_0^{\pi} \int_0^{2\pi} Y_{\ell}^2(\theta; \phi) \sin^2(\theta) d\theta d\phi}} \tag{E.4}$$

and P_{ℓ} is the Legendre function

$$P_{\ell}(n; m; u) = (1 - u^2)^{\frac{m}{2}} \frac{(1)^n}{2^n (n+1)} \frac{d^{m+n}}{du^{m+n}} (1 - u^2)^n \tag{E.5}$$

Due to the factor of $(-1)^n$ with half-integer n , the Legendre function is purely imaginary. Combined with the factor of i^{ℓ} of M_{ℓ} , the complex conjugate of our radial function is

$$\overline{R_{\ell}} = (-1)^{\ell} R_{\ell} \tag{E.6}$$

This means that also

$$\overline{K_{\ell}} = (-1)^{\ell} K_{\ell} \tag{E.7}$$

We note that an extra factor of i^{ℓ} is used in this paper compared to [9] to get consistency with (C.13).

Using numerical eigenvector-determination to find the transformation matrices j^m_i has its limits, due to the huge size of the matrices (2^k by 2^k matrices). Memory constraints thus limit the feasibility to a maximum of 43, on a PC with 512 Mb ram. The j^m_i states can however easily be expanded analytically on the $sr;sl$ states. To see this, note that the commutation relations (14) show that considered as 3-vectors both $JL = \frac{SL}{2}$ and $JR = \frac{SR}{2}$ satisfy the usual commutation relations for angular momentum operators

$$[J_x; J_y] = iJ_z \quad (\text{E.8})$$

Eigenstates of SR_2 and SL_2 are thus states with definite values of the z-component of JR and JL as well as of their absolute magnitude squared, $JR^2 = JL^2 = \frac{k}{2}(\frac{k}{2} + 1)$ where $k = 2m + 1$.

As the components of the JR and JL commute (equation (B.7)) we can, from simultaneous eigenstates of $JR^2; JR_z$ and $JL^2; JL_z$ construct eigenstates of their sum, $L = JR + JL = (J_{12}; J_{20}; J_{01})$, i.e. eigenstates of definite $L^2 = \ell(\ell + 1)$ and $L_z = m$, by the rule for vector addition of angular momentum [20]:

$$j^m_i = \sum_{srsl} \left(\ell; \frac{k}{2}; \frac{k}{2}; m; \frac{sr}{2}; \frac{sl}{2} \right) j^{srsl}_i \quad (\text{E.9})$$

This shows that the expansion coefficients between the eigenstates j^{srsl}_i of SR_2 and SL_2 and the eigenstates j^m_i of L^2 and $L_z = J_{01}$ are just Clebsch-Gordan coefficients, which have been worked out once and for all [20]. They are real when the relative phases are chosen by omitting the factor i in (27) and (28) which we will assume in the following.

With real Clebsch-Gordan coefficients, the inverse expansion of (E.9) reads:

$$j^{srsl}_i = \sum_m \left(\ell; \frac{k}{2}; \frac{k}{2}; m; \frac{sr}{2}; \frac{sl}{2} \right) j^m_i \quad (\text{E.10})$$

Inserting the expansion coefficients $cg_{srsl}^{k\ell} = \left(\ell; \frac{k}{2}; \frac{k}{2}; \frac{sr+sl}{2}; \frac{sr}{2}; \frac{sl}{2} \right)$ into the expression (C.13) we arrive at the following expression for the Y_m

$$Y_m(\theta; \phi) = \sum_{sr} N_{sr} cg_{sr}^{k\ell} cg_{sr}^{k\ell} e^{i sr} Y_m(\theta; \phi) \quad (\text{E.11})$$

Using the inverse expansion (E.10), we then find from (E.11) the following expression for the screw-eigenstates $h_j^{srsl}_i$:

$$h_j^{srsl}(\theta; \phi) = \sum_{sr^0} cg_{srsl}^{k\ell} N_{sr^0} cg_{sr^0}^{k\ell} cg_{sr^0}^{k\ell} e^{i sr^0} Y_m(\theta; \phi) \quad (\text{E.12})$$

where $m = \frac{sr+sl}{2}$.

Our group symmetrical functions can then be expressed using the equation (D.9). This enable us to determine the coefficients $a_{s_0}^{sr}$ by requiring the resulting function to be not only invariant to a right-screw along the z-axis, which was used in Appendix D to realise that the admissible sr values satisfy $sr = 0 \pmod{N}$ but also to another

specific Clifford-translation, which together with the translation along the z-axis spans the group Γ . For the group I we choose a translation of $\frac{0}{I} = \frac{1}{5}$ in the direction $(\frac{1}{5}; 0)$ and for the group T a translation of $\frac{0}{T} = \frac{1}{3}$ in the direction $(\frac{1}{3}; 0)$. For the group O we choose $\frac{0}{O} = \frac{1}{3}$ in the direction $(\frac{1}{3}; 0)$. This generalises a technique originally derived for S^3/I in [16], and for all three binary spaces in [17]. The invariance means that

$$\sum_{sr} a_{s^0}^{sr} \sum_{sl} \omega_{sr sl}^{k'} N_{sr} \omega_{sr^0}^{k_0} \omega_{sr^0}^{k'} (1 - e^{i \cdot 0 sr^0}) e^{i sr^0} Y_m(\frac{1}{3}; 0) \quad (E.13)$$

must be identically zero for all k . This requires all the coefficients in the Fourier-expansion in θ to vanish, i.e.

$$\sum_{sr} C_{sr}^{sr^0} a_{s^0}^{sr} = 0 \quad (E.14)$$

where

$$C_{sr}^{sr^0} = \sum_{sl} \omega_{sr sl}^{k'} N_{sr} \omega_{sr^0}^{k_0} \omega_{sr^0}^{k'} (1 - e^{i \cdot 0 sr^0}) Y_m(\frac{1}{3}; 0) \quad (E.15)$$

We can hence determine the $a_{s^0}^{sr}$ as the s^0 eigenvectors with eigenvalue zero, to the matrix $C^Y C$. Here sr only runs over $sr = 0 \pmod N$. As the result is independent of sl we can choose $sl = 0$ when doing the computation.

Using (D.9) and (E.12) we get the group symmetrical functions.

We do not in this paper actually use the functions as such, we only use their expansion for calculating the matrix elements of the group averaging operator.

Appendix F. The matrix elements $\langle k' m j k' \nu m^0 i \rangle$

From the results in the preceding sections we find that the matrix elements of the group averaging operator are

$$\begin{aligned} & \langle k' m j k' \nu m^0 i \rangle \\ &= \sum_{srs'l} \langle k' m j(\frac{1}{srs'l} k' sr sl) \rangle \sum_{s^0} \langle k' sl s^0 i \rangle \sum_{sr^0} \langle k' sr^0 sl j k' \nu m^0 i \rangle \\ &= \sum_{s^0} \sum_{srs'l} \langle k' m j k' sr sl \rangle a_{s^0}^{sr} \overline{a_{s^0}^{sr^0}} \langle k' sr^0 sl j k' \nu m^0 i \rangle \\ &= \sum_{s^0 sl} \sum_{srs'l} \omega_{2m}^{k'} a_{s^0}^{2m sl} \overline{a_{s^0}^{2m^0 sl}} \omega_{2m^0 sl}^{k'} \quad (F.1) \end{aligned}$$

Here the sum over sl should only be extended to values (if any) that satisfy $2m - sl = 2m^0 - sl = 0 \pmod N$.

Appendix G. Cosmic expectation value of C_ℓ

The starting point is the equation (14) in the methods section, giving the temperature as a function of angle in the sky. The equation as given, will normally, with complex random Gaussian variables X_s , result in a complex temperature signal, which is due to the fact that we work with complex eigenfunctions of the Laplacian. As the observed temperature is of course real, only the real part of the expression should be retained. Further, we have to take into account the chosen relative phases of our wavefunctions $h_{\ell j \ell m i}$, given in equation (E.2) and (E.7) of Appendix E. Hence we should write

$$2 T(\theta) = \sum_{\ell s} K_\ell Y_\ell(\theta) h_{\ell j \ell m i} X_s + c.c. \quad (G.1)$$

where $c.c.$ is the complex conjugate of the first expression, i.e. by (E.2) and (E.7)

$$c.c. = \sum_{\ell s} K_\ell Y_\ell(\theta) (1)^\ell h_{\ell j \ell m i} \overline{X_s} \quad (G.2)$$

Expanding on spherical harmonics

$$T(\theta) = \sum_{\ell} a_\ell Y_\ell(\theta) \quad (G.3)$$

We find

$$2a_\ell = \sum_s K_\ell [h_{\ell j \ell m i} X_s (1)^\ell h_{\ell j \ell m i} \overline{X_s}] \quad (G.4)$$

From this we get:

$$\begin{aligned} & 4a_\ell \overline{a_\ell} \\ &= \sum_{s_1 s_2} K_{\ell s_1} \overline{K_{\ell s_2}} \\ & \quad [h_{\ell j \ell m i} X_{s_1} (1)^\ell h_{\ell j \ell m i} \overline{X_{s_1}}] \\ & \quad [h_{\ell j \ell m i} \overline{X_{s_2}} (1)^\ell h_{\ell j \ell m i} X_{s_2}] \end{aligned} \quad (G.5)$$

Taking ensemble averages and summing over m , and using (7) in the methods section gives

$$\begin{aligned} 4 \sum_m a_\ell \overline{a_\ell} &= \sum_{\ell s} 2 K_\ell \sum_j h_{\ell j \ell m i} h_{\ell j \ell m i} \\ &= \sum_m \sum_{\ell s} 2 K_\ell \sum_j h_{\ell j \ell m i} h_{\ell j \ell m i} \end{aligned} \quad (G.6)$$

where G is the group averaging operator. Hence we have found the following expression for the cosmic ensemble average of the C_ℓ :

$$\langle C_\ell \rangle = \sum_m \frac{h_{\ell j \ell m i} \overline{h_{\ell j \ell m i}}}{2^\ell + 1} = \frac{1}{2} \sum_j K_\ell \sum_m \frac{h_{\ell j \ell m i} h_{\ell j \ell m i}}{2^\ell + 1} \quad (G.7)$$

We show in Appendix I that this may be further simplified to

$$\langle C_\ell \rangle = \frac{1}{2} \sum_j K_\ell \frac{\text{multiplicity}(\ell)}{2} \quad (G.8)$$

The significance of this relation, which is stated as a conjecture in [18], but in this paper is proven rigorously, is that it demonstrates that the spectrum can be computed solely from the radial wave function. The software used (Mathcad) allows to evaluate this sum up to $l = 101$. This limit arises from the fact that Mathcad's symbolic engine, which is used to expand the Legendre functions (E.5), produces exact rational coefficients with numerators and denominators that must be smaller than the largest real which is allowed in Mathcad. It is a possibility to be explored, that using instead the Fourier expansion (C.13) would allow this limit to be raised.

Appendix H. Cosmic variance of C_l

We use (G.4) and (E.7) to get

$$\begin{aligned}
 16a_m \overline{a_m} a_{l_1 l_2 l_3 l_4} \overline{a_{l_1 l_2 l_3 l_4}} = & \\
 (1)^{l_1+l_2+l_3+l_4} K_{l_1} K_{l_2} K_{l_3} K_{l_4} & \\
 \int_{-1}^1 \int_{-1}^1 \int_{-1}^1 \int_{-1}^1 dx_1 dx_2 dx_3 dx_4 & \\
 [h_{l_1}^m j_{l_1}^{s_1} iX_{l_1 s_1} (1)^m h_{l_1}^{s_1} j_{l_1}^{-m} i\overline{X_{l_1 s_1}}] & \\
 [h_{l_2}^{m^0} j_{l_2}^{s_2} iX_{l_2 s_2} (1)^m h_{l_2}^{-m} j_{l_2}^{s_2} iX_{l_2 s_2}] & \\
 [h_{l_3}^{m^0} j_{l_3}^{s_3} iX_{l_3 s_3} (1)^{m^0} h_{l_3}^{s_3} j_{l_3}^{m^0} i\overline{X_{l_3 s_3}}] & \\
 [h_{l_4}^{s_4} j_{l_4}^{m^0} i\overline{X_{l_4 s_4}} (1)^{m^0} h_{l_4}^{m^0} j_{l_4}^{s_4} iX_{l_4 s_4}] & \quad (H.1)
 \end{aligned}$$

When we thereafter take the ensemble average, the random variables only contribute in pairs (see (8) in the methods section). Doing the pairing between variables in the first and second factor, and between the third and fourth factor just result in the product $16a_m \overline{a_m} i h_{l_1}^{s_1} a_{l_1 l_2 l_3 l_4} \overline{a_{l_1 l_2 l_3 l_4}} i$, while the other possible pairings produce

$$\begin{aligned}
 & (1)^{l_1+l_2} K_{l_1} K_{l_1} K_{l_2} K_{l_2} \\
 & [(1)^{m^0} h_{l_1}^m j_{l_1}^{s_1} j_{l_1}^{m^0} i (1)^m h_{l_1}^{m^0} j_{l_1}^{s_1} j_{l_1}^{-m} i] \\
 & [(1)^{m^0} h_{l_2}^{m^0} j_{l_2}^{s_2} j_{l_2}^{m^0} i (1)^m h_{l_2}^{-m} j_{l_2}^{s_2} j_{l_2}^{m^0} i] \\
 + & (1)^{l_1+l_2} K_{l_1} K_{l_1} K_{l_2} K_{l_2} \\
 & [h_{l_1}^m j_{l_1}^{s_1} j_{l_1}^{m^0} i + (1)^{l_1+l_2} h_{l_1}^{m^0} j_{l_1}^{s_1} j_{l_1}^{-m} i] \\
 & [h_{l_2}^{m^0} j_{l_2}^{s_2} j_{l_2}^{m^0} i + (1)^{l_1+l_2} h_{l_2}^{-m} j_{l_2}^{s_2} j_{l_2}^{m^0} i] \quad (H.2)
 \end{aligned}$$

One should note, that the matrix elements of G are real for all the manifolds we study in this paper, and hence also symmetric (this may be shown strictly), a fact we do not exploit here. Summing over m and m^0 we realise by substitution of m^0 for m^0 that the two sums gives identical contributions. Further, the first factor is the complex conjugate

of the second (albeit real), with ℓ_1 substituted for ℓ_2 . Our final result becomes then that the covariance of C_ℓ is

$$Q_{\ell_1 \ell_2} = \langle C_{\ell_1} C_{\ell_2} \rangle = \langle C_{\ell_1} i C_{\ell_2} \rangle = \frac{1}{2} \frac{1}{2\ell_1 + 1} \frac{1}{2\ell_2 + 1} \sum_{m m_0} X_{m m_0} M_{m m_0}^{(\ell_1 \ell_2)} \quad (H.3)$$

where the matrix M is derived by "symmetrizing" the sum of the matrix elements of the group averaging operator, as follows:

$$M_{m m_0}^{(\ell_1 \ell_2)} = \sum_{K, K'} \frac{\langle h_{\ell_1 m} \mathcal{G}_{\ell_2} j^0 m_0 | (1)^{\ell_1 + \ell_2 + m + m_0} h_{\ell_1 m} \mathcal{G}_{\ell_2} j^0 m_0 \rangle}{2} \quad (H.4)$$

We note that all the elements of the covariance matrix are non-negative.

For S^3 the matrix $\langle h_{\ell_1 m} \mathcal{G}_{\ell_2} j^0 m_0 | h_{\ell_1 m} \mathcal{G}_{\ell_2} j^0 m_0 \rangle = \delta_{m m_0}$ so that the variance is just

$$Q_{\ell_1 \ell_2} = \delta_{\ell_1 \ell_2} \frac{2}{2\ell_1 + 1} \langle C_{\ell_1}^2 \rangle \quad (H.5)$$

Appendix I. The formula for the spectrum

In the Appendix F we claimed that the formula for the C_ℓ of equation (G.7) may be simplified to the expression of equation (G.8).

The starting point is equation (G.7), which may further be simplified by introducing the projection operator on the ℓ -eigenspace $P(\ell) = \sum_{m, m_0} | \ell m \rangle \langle \ell m |$

$$(2\ell + 1) \langle C_{\ell} \rangle = \sum_{K, K'} \frac{K_{\ell} \cdot j_{\ell}^2}{2} \text{trace}[G P(\ell)] \quad (I.1)$$

This, as we demonstrate just below, boils down to

$$\langle C_{\ell} \rangle = \sum_{K, K'} \frac{K_{\ell} \cdot j_{\ell}^2}{2} \frac{\text{multiplicity}(\ell)}{2} \quad (I.2)$$

This equation is very convenient, as it allows us to calculate the spectrum without calculating the eigenfunctions which are symmetrical under the holonomy of the manifold considered. The result holds for all manifolds with holonomies that are Clifford-translations.

For S^3 we get just

$$\langle C_{\ell} \rangle = \sum_{K, K'} \frac{K_{\ell} \cdot j_{\ell}^2}{2} \quad (I.3)$$

The steps leading from equation (I.1) to (I.2) are based on the observation that both G , the group averaging operator and P_ℓ , the operator that projects on the eigenspace belonging to the eigenvalue $\ell(\ell + 1)$ of the angular momentum, has certain symmetries.

First we note that G is a sum of right-screw transformations, and hence commutes with all left-screw transformations, and therefore also with the generator SL_2 of such transformations in the wz,xy direction:

$$SL_2 G G SL_2 = 0 \tag{I.4}$$

It then follows easily, that the matrix elements of G between eigenstates of SR_2 and SL_2 are diagonal in sl , because:

$$\begin{aligned} sl hslsr jG jsl^0sr^0i &= hslsr jSL_2 G jsl^0sr^0i \\ &= hslsr jG SL_2 jsl^0sr^0i = sl^0 hslsr jG jsl^0sr^0i \end{aligned} \tag{I.5}$$

and therefore:

$$hslsr jG jsl^0sr^0i = hslsr jG jslsr^0i_{slsl^0} \tag{I.6}$$

Further, the operator AL_2 for lifting sl also commutes with G from which we by standard arguments can conclude that the diagonal elements are independent of sl . By construction:

$$AL_2 jslsri = al(sl) jsl+ 2sri \quad hslsr jAL_2^y = \overline{al(sl)} hsl+ 2srj \tag{I.7}$$

Noting that AL_2^y acting on the state $jsl+ 2sri$ is proportional to $jsl sri$ and that, by complex conjugation

$$hsl+ 2srjAL_2 jslsri = al(sl) \quad hslsr jAL_2^y jsl+ 2sri = \overline{al(sl)} \tag{I.8}$$

we see that

$$AL_2^y jsl+ 2sri = \overline{al(sl)} jslsri \quad hsl+ 2srjAL_2 = al(sl)hslsrj \tag{I.9}$$

From (I.7) and (I.8) follows

$$\begin{aligned} al(sl)hsl+ 2srjG jsl+ 2sri &= hsl+ 2srjG AL_2 jsl+ 2sri \\ &= hsl+ 2srjAL_2 G jsl+ 2sri = al(sl)hslsrjG jslsri \end{aligned} \tag{I.10}$$

demonstrating that the diagonal matrix elements of G are independent of sl .

As the trace of G is equal to the dimension of the space of non-vanishing symmetrical states, i.e. the multiplicity, we find that, for each of the values of sl :

$$\sum_{sr} hslsr jG jslsri = \frac{1}{slsr} \sum_{slsr} hslsr jG jslsri = \frac{\text{multiplicity}(\)}{slsr} \tag{I.11}$$

For the operator P , we find, firstly, that the only nonzero matrix elements are the ones satisfying the selection rule $sl+ sr = sl^0+ sr^0$ and secondly, although not so easily, that the sum

$$\sum_{sl} hslsr jP \cdot jsr sli \tag{I.12}$$

is independent of sr and hence for each of the values of sr must be:

$$\sum_{sl} hslsr jP \cdot jsr sli = \frac{1}{slsr} \sum_{slsr} hslsr jP \cdot jsr sli = \frac{2^l + 1}{slsr} \tag{I.13}$$

Combining the two equations, we realise that

$$\begin{aligned} \text{trace}(G P_1) &= \sum_{s_l s_r s_l^0 s_r^0} \text{hslsr } jG \text{ } j s_l^0 s_r^0 i \text{hsl}^0 s_r^0 jP, j s_l s_r i \\ &= \sum_{s_l s_r} \text{hslsr } jG \text{ } j s_l s_r i \text{hslsr } jP, j s_l s_r i \end{aligned} \quad (\text{I.14})$$

because equation (77) requires $s_l = s_l^0$ and the selection rule for P , then $s_r = s_r^0$, which by the independence of the G term on s_l allow us to write

$$\begin{aligned} \text{trace}(G P_1) &= \sum_{s_r} \text{hslsr } jG \text{ } j s_l s_r i \sum_{s_l} \text{hslsr } jP, j s_l s_r i \\ &= \frac{\text{multiplicity}(\) 2^l + 1}{} \end{aligned} \quad (\text{I.15})$$

which finishes our proof, apart from proving the above stated properties of P .

To do that, first note that $SR_2 + SL_2$ is just $2 J_{01}$ and hence commutes with P . Therefore

$$(s_l + s_r) \text{hslsr } jP, j s_l^0 s_r^0 i = (s_l^0 + s_r^0) \text{hslsr } jP, j s_l^0 s_r^0 i \quad (\text{I.16})$$

showing that if $(s_l + s_r) \notin (s_l^0 + s_r^0)$ the matrix element vanishes.

The further remaining detail, of showing independence of $\sum_{s_l} \text{hslsr } s_l jP, j s_r s_l i$ of s_r is accomplished by noting that the operator $AL_2 + AR_2$ is just $2 (J_{01} + iJ_{20})$ and hence commutes with P .

We use this to evaluate

$$\text{hslsr} + 2 jP, (AL_2 + AR_2) j s_l s_r i = \text{hslsr} + 2 j (AL_2 + AR_2) P, j s_l + 2 s_r i \quad (\text{I.17})$$

Noting that we have equations for the action of AR_2 analogous to the above for AL_2 , we find, by letting $AL_2 + AR_2$ act to the right on the ket in the first expression, and to the left on the bra in the second

$$\begin{aligned} & a_l(s_l) \text{hslsr} + 2 jP, j s_l + 2 s_r i + a_r(s_r) \text{hslsr} + 2 jP, j s_l s_r + 2 i \\ &= a_l(s_l - 2) \text{hsl} - 2 s_r + 2 jP, j s_l s_r i + a_r(s_r) \text{hslsr } jP, j s_l s_r i \end{aligned} \quad (\text{I.18})$$

Next we sum over s_l , and note that in doing that, we can replace the $s_l - 2$ in the first term on the right hand side of the equation with s_l (we can do that, because $a_l(s_l)$ is zero when s_l is the maximum value $s_{l, \text{max}} = \dots - 1$). The sum of this term then equals the sum of the first term on the left hand side, and both sums can be neglected. We are left with the sums over the second terms

$$\sum_{s_l} a_r(s_r) \text{hslsr} + 2 jP, j s_l s_r + 2 i = \sum_{s_l} a_r(s_r) \text{hslsr } jP, j s_l s_r i \quad (\text{I.19})$$

which demonstrates that the sum is independent of s_r which completes the proof.

Appendix J. Likelihood function

Central to extracting uncertainty-bounds for the cosmological parameters from the observed properties of the CMB is the setting up of a likelihood function. In the case of flat space, or S^3 models, this is relatively straightforward, as the a_m 's can be considered to be independently distributed random Gaussian variables, so that the C_l 's have a chi-square distribution with $2l+1$ degrees of freedom.

In the case of a nontrivial global topology for the universe, as the $S^3=I$, $S^3=O$ and $S^3=T$ studied here, the situation is more complicated.

The C_l 's are then definitely not chi-square distributed, and the C_l 's are not independent.

One may in principle calculate the likelihood distributions from the assumed Gaussian distributions of the random amplitudes X by a large number of simulations, for each choice of the cosmological parameters. Such grid-based approaches are very demanding in terms of computer-time.

The strategy used by the WMAP team, for nearly flat models, is instead to sample the cosmological parameter-space by setting up Markov chain Monte-Carlo simulations [15]. That approach is critically dependent on the ability to specify the conditional probability distribution for the observations, given the model, which is a simple task when the C_l 's are chi-square-distributed, but not feasible in the case of S^3 .

In this preliminary analysis it was chosen to use a crude approximation instead, by assuming the C_l 's to have the Gaussian distribution of (J.1).

From the ensemble-averages of Appendix G and Appendix H for the C_l 's and their covariance, such a multidimensional Gaussian distribution is easily constructed from the covariance matrix Q of (H.3):

$$W(C_l^{\text{obs}} | \text{model}) = \frac{1}{\det(2Q^{\text{th}})} e^{-\frac{1}{2} \sum_{l_1, l_2} (C_{l_1}^{\text{obs}} - C_{l_1}^{\text{th}})(C_{l_2}^{\text{obs}} - C_{l_2}^{\text{th}}) Q_{l_1 l_2}^{\text{th}}} \quad (\text{J.1})$$

Here the probability depends on the model parameters through the dependence of C_l^{th} and Q^{th} on the "theory", i.e. the model parameters. In a more refined analysis, one has to consider the variance due to measurement uncertainties, but for the low- l power, which we consider here, the cosmological variance dominates. Hence we ignore the complications of measurement uncertainty in the present analysis.

Often a prior is applied, i.e. an a priori distribution $P^{\text{ante}}(\text{model})$ for the model parameters, which may be as simple as to constrain the parameters to a certain window

in parameter space. In any case, application of Bayes principle result in the following likelihood function for the model parameters, given the observed C_i 's:

$$L(\text{model} | C_i^{\text{obs}}) = \frac{W(C_i^{\text{obs}} | \text{model}) P^{\text{ante}}(\text{model})}{\int_{\text{model}} W(C_i^{\text{obs}} | \text{model}) P^{\text{ante}}(\text{model})} \quad (\text{J.2})$$

Two different a priori distributions are used in this paper: a uniform prior over the cosmic window studied, and a Gaussian prior with means and standard deviations corresponding to the WMAP estimate for the parameters, $\sigma_{\text{mass}} = 0.257 + \dots = 0.025$ and the general estimate [3] of $\sigma_{\text{tot}} = 1.02 + \dots = 0.02$.

It's a valid question to ask, how good the ansatz (J.1) is. It's clearly unphysical, in as much as the C_i 's are inherently positive. It's also known to be slightly biased [15], in the case of S^3 where the exact distribution is

$$W_{S^3}(C_i^{\text{obs}} | \text{model}) = \prod_{i=1}^Y (C_i^{\text{obs}}; C_i^{\text{th}}; Q_i^{\text{th}}) \quad (\text{J.3})$$

ie. a product of chi-square distributions with mean $\langle C_i^{\text{obs}} \rangle = C_i^{\text{th}}$ and $2\chi^2 + 1 = 2 C_i^{\text{th}^2} = Q_i^{\text{th}}$ degrees of freedom. However, the distribution (J.1) has the proper mean values, if we neglect that the C_i 's are inherently positive, for all the manifolds S^3 / \dots , derivable from the theoretical relations of the preceding sections:

$$\begin{aligned} \langle C_i^{\text{obs}} \rangle &= C_i^{\text{th}} \\ \langle C_i^{\text{obs}} C_j^{\text{obs}} \rangle &= \langle C_i^{\text{obs}} \rangle \langle C_j^{\text{obs}} \rangle + \langle C_i^{\text{obs}} C_j^{\text{obs}} \rangle - \langle C_i^{\text{obs}} \rangle \langle C_j^{\text{obs}} \rangle = Q_{ij}^{\text{th}} \\ \langle R^2 \rangle &= \sum_{i,j=0}^X (C_i^{\text{obs}} - C_i^{\text{th}})(C_j^{\text{obs}} - C_j^{\text{th}}) Q_{ij}^{\text{th}^{-1}} = 14 \end{aligned} \quad (\text{J.4})$$

where the sum over i and j runs from 2 to 15.

Doing a direct simulation of (J.4), for an ensemble of 10.000 Universes, which takes about 20 minutes calculation time for each choice of cosmological parameters, the resulting distributions for the C_i 's can be found, and they are reasonably approximated by chi-square distributions, with an effective degree of freedom of $D = 2 C_i^{\text{th}^2} = Q_i^{\text{th}}$, with some exceptions, however, as seen in Figure J3. As an alternative to (J.1) the following 2 probability functions have been tested:

$$W(C_i^{\text{obs}} | \text{model}) = \prod_{i=1}^Y (C_i^{\text{obs}}; C_i^{\text{th}}; Q_i^{\text{th}}) \quad (\text{J.5})$$

which means that the off-diagonal elements of Q^{th} are simply neglected, as well as the distribution:

$$W(C_i^{\text{obs}} | \text{model}) = \det P \prod_{i=1}^Y (C_i^{\text{obs}}; C_i^{\text{th}}; 1) = \det P \prod_{i=1}^Y (P C_i^{\text{obs}}; P C_i^{\text{th}}; 1) \quad (\text{J.6})$$

where the matrix P is used to get a unit covariance matrix:

$$C_i^{\text{obs}} = P C_i^{\text{obs}} \quad C_i^{\text{th}} = P C_i^{\text{th}} \quad P^0 P = Q^{\text{th}^{-1}} \quad (\text{J.7})$$

The function (J.6) has the proper mean values (J.4) whereas this is not the case for the function (J.5).

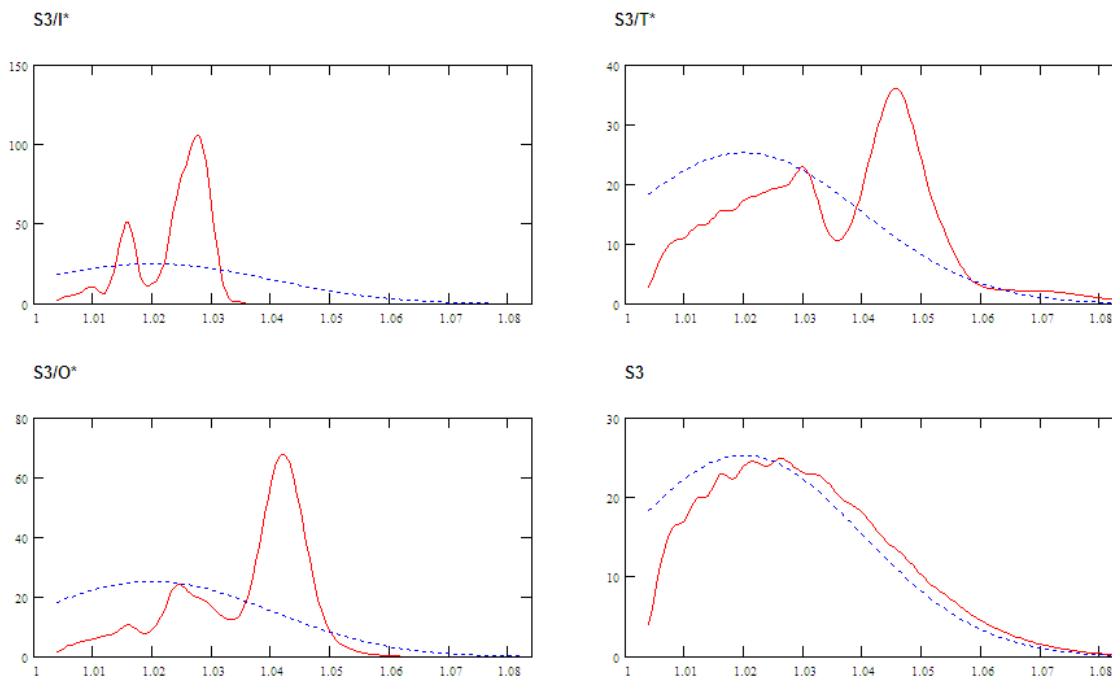


Figure J1. The likelihood distribution as a function of τ_{tot} along the most likely value of $m_{ass} = 0.26$ for $S^3=O$, $S^3=T$, $S^3=I$ and $S^3=$ with the probability function (J.5). Compare with Figure 2 of section 3. Dotted line shows the prior distribution, for comparison. Note the different scales on the vertical axes.

Figure J1 and Figure J2 illustrate, that the choice of the probability function W has an impact on the calculated ex post likelihood surfaces. Using (J.5) or (J.6) rather than (J.3) has the effect, that the secondary optimum for $S^3=I$ near $\tau_{tot} = 1.017$ becomes somewhat larger, but still smaller, than the peak near $\tau_{tot} = 1.030$. Also the peak at 1.03 shifts slightly towards lower values of τ_{tot} . Hence, the issue of establishing a proper probability function W remains an important question for examining the best estimates for the cosmological parameters in case of the nontrivial topologies $S^3=$.

Neither of the proposed distributions W are exact. Hence the proper solution in future work could be to use that the a_m 's do in fact have a multidimensional Gaussian distribution, which can be expressed by the covariance matrix $Q_{m_i m_j} = \langle a_{m_i} a_{m_j} \rangle$. The input to the likelihood calculation would then need to be the observed a_m 's instead of the observed C 's. This approach would be complicated by the anisotropy of the a_m 's which are found for all the non-trivial topologies $S^3=$, as the theoretical ensemble averages of $\langle a_{m_i} a_{m_j} \rangle$ depend on the alignment of the special directions. If these directions can be found by a matching circle's detection, the procedure could be used quite straightforwardly, however, to get an improved estimate of the cosmological parameters. Another intriguing possibility, in case the matched circles search does not produce a definite answer, could be that a systematic rotation in the 3-parameter space of rotations on the sky of the a_m 's, although computationally challenging, could yield

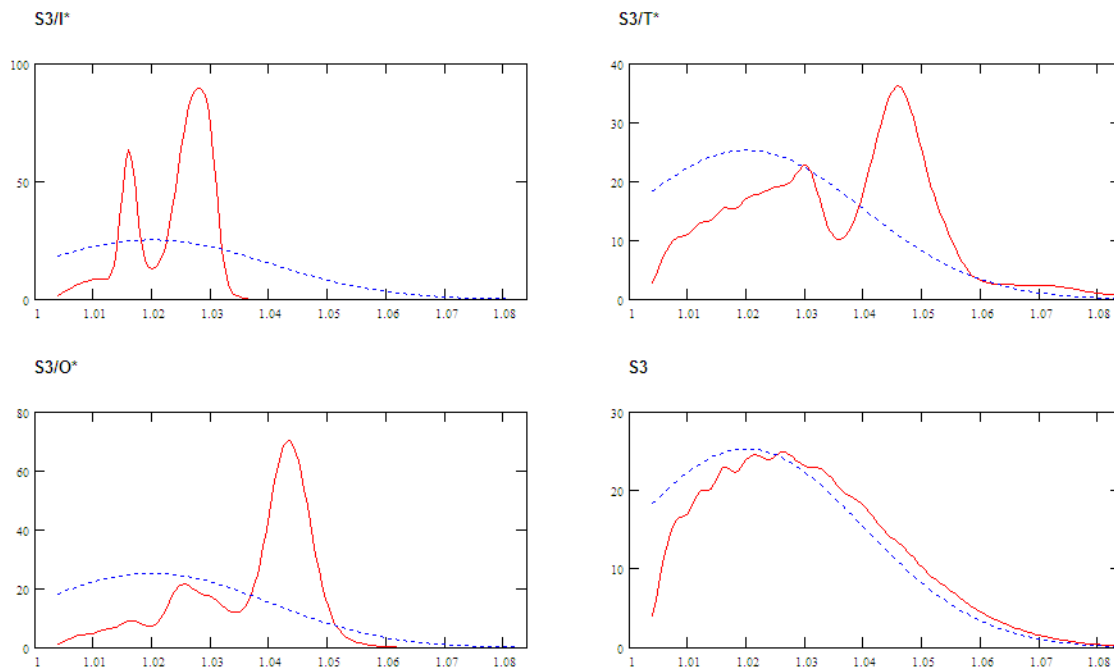


Figure J2. The likelihood distribution as a function of t_{tot} along the most likely value of $m_{ass} = 0.26$ for $S^3=O$, $S^3=T$, S^3 and $S^3=I$, with the probability function (J.6). Compare with Figure 2 of section 3. Dotted line shows the prior distribution, for comparison. Note the different scales on the vertical axes.

a best fit alignment between observations and theory, thus identifying any preferred cosmic directions, even without recourse to finding matching circles.

It's rather easy to derive, that (J.1) implies that the last quantity R^2 is distributed as $(R^2; 14; 14)$, for all the manifolds $S^3/$. This may be compared with the exact distribution of R^2 for $S^3=I$ derivable by simulation from (G.4), shown in Figure J4.

It is seen that such a chi-square distribution does not reproduce the simulated distribution of R^2 fairly well, for the case of $S^3=I$. For the more general manifolds such as $S^3/$ we do not, however, have an explicit, exact expression for the true multidimensional distribution $W(C^{obs}; j; model)$ (but it could be simulated by drawing a large number of the random variables X_{is}).

Nevertheless, as the distribution (J.1) does reproduce the mean values (J.4) if we can neglect that the C_i 's are positive, we will assume that (J.1) is a workable approximation, at this preliminary state of analysis.

A significant lesson from Figure J4 is, that the statistics R^2 , which is the sum of the squared deviation of the observed C_i 's from their cosmological ensemble averages, measured relative to the expected variance, is a fairly broad distribution. As it is further

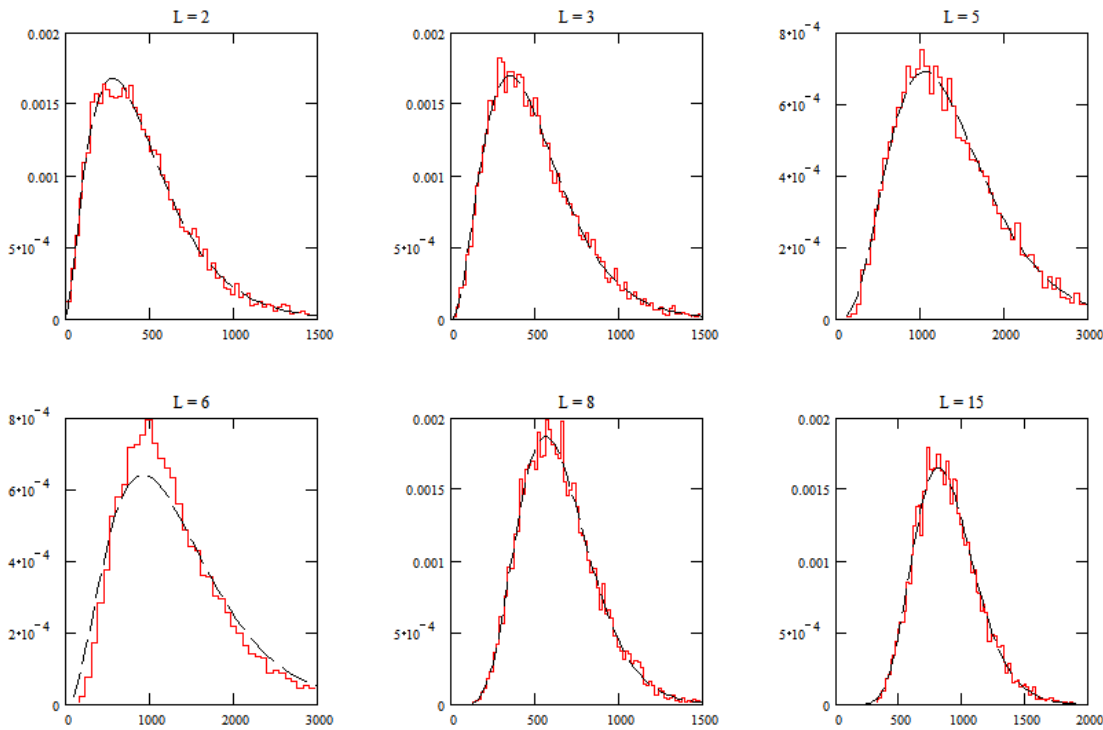


Figure J3. The simulated histograms for $S^3=I$ of the moments $\langle l+1 \rangle C_{l,2}$ for selected l -values (calculated for $m_{\text{ass}} = 0.26$ and $t_{\text{tot}} = 1.028$). The dashed lines show chi-square distributions with the same mean and variance as the histograms. The simulated distributions are clearly not chi-square, especially for $l = 6$ and possibly for $l = 2$.

found, that the observed value of R^2 is fairly close to its expected value of 14, for all topologies and across the cosmological parameter space, we can not use R^2 as a statistic to reject any specific topology, or any choice of the cosmological parameters.

Whereas the distribution (J.1) is very sensitive to deviations of $C_{l,2}^{\text{obs}}$ from $C_{l,2}^{\text{th}}$ this is not the case for the distribution of R^2 because of the "phase space factor", i.e. the fact that the surface to radius ratio in the 14-dimensional space of the $C_{l,2}$'s grows quickly with R . This means, that we can use the likelihood distribution (J.1) to pinpoint the best values of the cosmological parameters, given the topology, but cannot easily use it to discriminate between alternative topologies.

Appendix K. 2-point angular correlation function

The 2-point angular correlation function $C(\theta)$ is defined as the average over the sky of $C(\theta) = \text{av}(\mathbf{T}(\hat{n}) \cdot \mathbf{T}(\hat{n}'))$ with $\hat{n} \cdot \hat{n}' = \cos(\theta)$, which is related to the moments $C_{l,2}$ by

$$C(\theta) = \frac{1}{4\pi} \sum_{l=2}^{\infty} (2l+1) C_{l,2} P_l(\cos(\theta)) \tag{K.1}$$

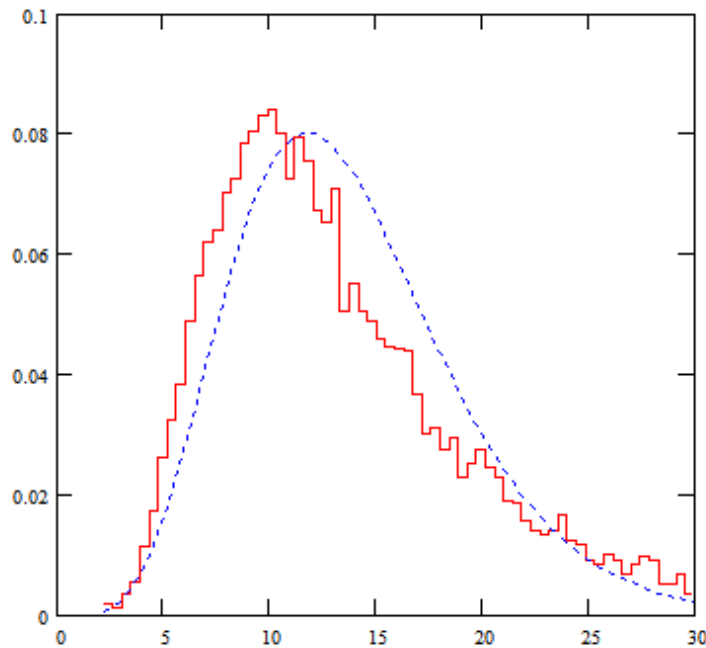


Figure J4. The simulated histogram for $S^3=I$ of the R^2 defined by (J.4), calculated for $m_{\text{ass}} = 0.26$ and $t_{\text{tot}} = 1.028$ and 10,000 universes. Horizontal axis is R^2 . The simulated distribution is not chi-square, with 14 degrees of freedom, showing that the ansatz (J.1) is not perfect.

where P_ν is the Legendre function. The cosmic expectation value of $C(\theta)$ is found by replacing C_ν with $\langle C_\nu \rangle$ and similarly, the cosmic variance of $C(\theta)$ is

$$\langle C(\theta) \rangle^2 - \langle C(\theta) \rangle^2 = \frac{1}{(4\pi)^2} \sum_{\ell=2}^{\infty} \sum_{m=0}^{\ell} (2\ell+1)(2\ell+1) Q_{\ell m} P_\ell(\cos(\theta)) P_{\ell m}(\cos(\theta)) \quad (K 2)$$

As discussed in [3] the observed two-point correlation function is very flat for large angles, a feature which the Λ CDM models based on flat space or nearly flat space are unable to reproduce. The anomaly is mainly a result of the very low observed quadrupole and octopole moments. To quantify the anomaly, simulations are reported of the statistic

$$S(\theta) = \frac{\int_0^{\cos(\theta)} C(\theta')^2 d\cos(\theta')}{1} \quad (K 3)$$

It is found, for the best fit Λ CDM model, for $\theta = 60$ degrees that only 0.15% of the simulations have lower value than the observed value of $S(\theta)$. For the running index model, the similar result of simulations is found to be 0.3%.

In this paper, we only study the S-statistic filtered to a maximum value of ℓ of 15, but the results are quite similar as the S-statistic heavily emphasises the lowest multipoles. As an example, it is found that for $m_{\text{ass}} = 0.26$ and $t_{\text{tot}} = 1.028$ (the favoured value from this study) the S^3 model with a power law spectrum, gives an $S(60)$ lower than the observed value only in 0.13% of simulations. This is in contrast with simulations for $S^3=I$ where the simulations performed, for the same values of the

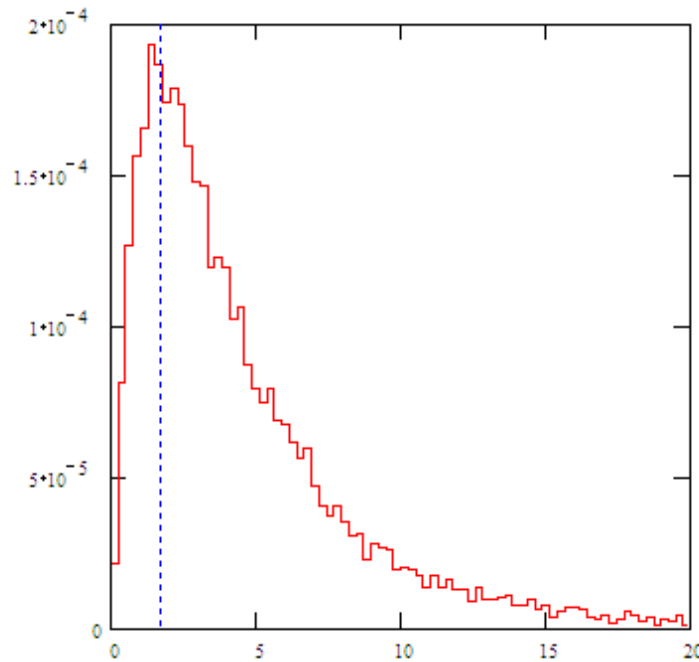


Figure K 1. The simulated histogram for $S^3=I$ of the $S(60)$ statistic, calculated for $m_{\text{ass}} = 0.26$ and $t_{\text{tot}} = 1.028$ and 10.000 universes. Horizontal axis is $S(60)$ times 10^3 . The vertical line shows the observed value. The probability of getting a value less than the observed is 23%. The simulated distribution is not chi-square, but disregarding this one finds the effective degrees of freedom $2m_{\text{eff}} = \text{variance}$ to be 226, showing that the statistic is sampling very few random variables.

cosmological parameters, give a 23% chance of a lower $S(60)$ than observed, see Figure K 1.

In [18] the cosmological expectation value of the S -statistic is used to locate the values of the cosmological parameters that brings this expectation value closest to the observed value.

This might be problematic, however, because the choice of statistics is heavily biased to emphasize the low values of the two first multipole moments seen in the observations, as discussed in [14]. For that reason, it was preferred in this paper, rather to use the maximum likelihood principle, even though it is based on only an approximate distribution W , to search for the most likely values in cosmological parameter space for each of the topologies. As shown in Figure 1 and Figure 2 the maximum likelihood is found for $m_{\text{ass}} = 0.26$ and $t_{\text{tot}} = 1.028 \pm 0.0023$. A secondary but smaller peak, however, is found near the value of t_{tot} found in [18] by minimizing the S -statistic. The center value and width of this peak yields $t_{\text{tot}} = 1.017 \pm 0.0015$. As shown in Figure J1 and Figure J2 this secondary peak becomes somewhat more pronounced when using the alternative approximate distributions (J.5) or (J.6).

References

- [1] G. Hinshaw et al, "Band power spectra in the COBE DMR four-year anisotropy maps" *Astrophys. J. Lett.* 464 (1996) L17 [astro-ph/9601058].
- [2] C. L. Bennett et al, "First year Wilkinson Microwave Anisotropy Probe (WMAP 1) observations: preliminary maps and basic results", *Astrophys. J. Suppl.* 148 (2003) 1{27 [astro-ph/0302207].
- [3] D. N. Spergel et al, "First year Wilkinson Microwave Anisotropy Probe (WMAP 1) observations: determination of cosmological parameters", *Astrophys. J. Suppl.* 148 (2003) 175{194 [astro-ph/0302209].
- [4] J. Levin, "Topology and the cosmic microwave background", *Phys. Rep.* 365 (2002) 251{333 [gr-qc/0108043].
- [5] J.-P. Luminet, J. Weeks, A. Riazuelo, R. Lehoucq and J.-P. Uzan, "Dodecahedral space topology as an explanation for weak wide-angle temperature correlations in the cosmic microwave background", *Nature* 425 (2003) 593{595 [astro-ph/0310253].
- [6] J. Weeks, "The Poincaré dodecahedral space and the mystery of the missing fluctuations", *Notices of the Amer. Math. Soc.* 51 (2004) 610{619.
- [7] D. J. Schwarz, G. D. Starkman, D. Huterer and C. J. Copi, "Is the low- l microwave background cosmic?", *Phys. Rev. Lett.* 93 (2004) 221301, [astro-ph/0403353].
- [8] F. K. Hansen, A. J. Banday and K. M. Gorski, "Testing the cosmological principle of isotropy: local power spectrum estimates of the WMAP data", *MNRAS* 354, 3, 641{665 [astro-ph/0404206].
- [9] A. Riazuelo et al, "Simulating Cosmic Microwave Background maps in multi-connected spaces", *Physical Review D* 69 (2003) article 103514 [astro-ph/0212223].
- [10] R. Aurich et al, "Hyperbolic universes with a Homed Topology and the CMB Anisotropy", *Class. Quantum Grav.* 21 (2004) 4901{4926 [astro-ph/0403597].
- [11] R. Lehoucq et al, "Eigenmodes of 3-dimensional spherical spaces and their application to cosmology", *Class. Quantum Grav.* 19 (2002) 4683{4708 [gr-qc/0205009].
- [12] E. Gaussmann, R. Lehoucq, J.-P. Luminet, J.-P. Uzan and J. Weeks, "Topological lensing in spherical spaces", *Class. Quantum Grav.* 18 (2001) 5155-5186 [gr-qc/0106033].
- [13] P. A. M. Dirac, "The Principles of Quantum Mechanics", (Oxford at the Clarendon Press, 1958, 4th ed.).
- [14] G. Efsthathiou et al, "The Statistical Significance of the Low CMB Multipoles", *Mon. Not. R. Astron. Soc.* 346 (2003) L26 [astro-ph/0306431].
- [15] L. Verde et al, "First Year Wilkinson Microwave Anisotropy Probe (WMAP) 1 Observations: Parameter Estimation Methodology", *Astrophysical Journal Supplement Series* 148 (2003) 195{214
- [16] M. Lachize-Rey, "Eigenmodes of Dodecahedral space", *Class. Quantum Grav.* 21 (2004) 2455{2464 [gr-qc/0402035].
- [17] M. Lachize-Rey and S. Caillerie, "Laplacian eigenmodes for spherical spaces" *Class. Quantum Grav.* 22 (2005) 695-708
- [18] R. Aurich et al, "CMB Anisotropy of the Poincaré Dodecahedron", *?? NN* (2004) 1{26 [astro-ph/0412569].
- [19] P. Kramer, "Invariant operator due to F. Klein quantizes H. Poincaré's dodecahedral 3-manifold", *?? NN* (2004) 1{29 [gr-qc/0410094].
- [20] L. D. Landau and M. E. Lifshitz, "Quantum Mechanics", (Pergamon Press, Oxford, 1977, 3rd ed.).